Studies on the Effects of High Renewable Penetrations on Driving Point Impedance and Voltage Regulator Performance

National Renewable Energy Laboratory/ Sacramento Municipal Utility District Load Tap Changer Driving Point Impedance Project

Adarsh Nagarajan and Michael Coddington
National Renewable Energy Laboratory

David Brown, Sheikh Hassan,
Leonardo Franciosa, and Elaine Sison-Lebrilla
Sacramento Municipal Utility District

NREL is a national laboratory of the U.S. Department of Energy
Office of Energy Efficiency & Renewable Energy
Operated by the Alliance for Sustainable Energy, LLC

This report is available at no cost from the National Renewable Energy Laboratory (NREL) at www.nrel.gov/publications.

Technical Report
NREL/TP-5D00-70517
January 2018

Contract No. DE-AC36-

Studies on the Effects of High Renewable Penetrations on Driving Point Impedance and Voltage Regulator Performance

National Renewable Energy Laboratory/ Sacramento Municipal Utility District Load Tap Changer Driving Point Impedance Project

Adarsh Nagarajan and Michael Coddington
National Renewable Energy Laboratory

David Brown, Sheikh Hassan,
Leonardo Franciosa, and Elaine Sison-Lebrilla
Sacramento Municipal Utility District

NREL is a national laboratory of the U.S. Department of Energy
Office of Energy Efficiency & Renewable Energy
Operated by the Alliance for Sustainable Energy, LLC

This report is available at no cost from the National Renewable Energy Laboratory (NREL) at www.nrel.gov/publications.

National Renewable Energy Laboratory
15013 Denver West Parkway
Golden, CO 80401
303-275-3000 • www.nrel.gov

Technical Report
NREL/TP-5D00-70517
January 2018

Contract No. DE-AC36-

NOTICE

This report is available at no cost from the National Renewable Energy Laboratory (NREL) at www.nrel.gov/publications.

Available electronically at SciTech Connect http:/www.osti.gov/scitech

Available for a processing fee to U.S. Department of Energy and its contractors, in paper, from:

U.S. Department of Energy
Office of Scientific and Technical Information
P.O. Box 62
Oak Ridge, TN 37831-0062
OSTI http://www.osti.gov
Phone: 865.576.8401
Fax: 865.576.5728
Email: reports@osti.gov

Available for sale to the public, in paper, from:

U.S. Department of Commerce
National Technical Information Service
5301 Shawnee Road
Alexandria, VA 22312
NTIS http://www.ntis.gov
Phone: 800.553.6847 or 703.605.6000
Fax: 703.605.6900
Email: orders@ntis.gov

List of Acronyms

DER	Distributed energy resources
DPI	Driving point impedance
LTC	Load tap changer
PV	Photovoltaic
SMUD	Sacramento Municipal Utility District
XML	Extensible Markup Language

Executive Summary

This project explored the role of controllers—load tap changers (LTCs) and line regulators—on distribution feeders with increased distributed energy resources (DERs). Distribution feeders are facing a steep increase in DER penetration from specific classes of devices, including photovoltaic (PV) generators, energy storage systems, and demand response. Line regulators and LTCs represent a subset of control devices on distribution feeders used to regulate voltage delivered to customer locations. These devices operate in discrete steps, with each step changing the tap rate by 0.625% (hence a 10% change requires 16 steps).

Before DERs were introduced, power flow in a distribution feeder was unidirectional, i.e., from the substation to loads. Additionally, a predictable loading pattern that peaks in the afternoons or evenings and dips during nighttime made the operation of voltage regulators easier and understandable.

However, with increased penetration of renewable generation on distribution feeders, including homeowners installing solar panels on rooftop and additional utility-scale or commercial PV installations, a paradigm shift is occurring in the operational expectations of voltage regulators and LTCs. It has become very common to expect reverse power flows to the substation as a result of increased PV penetration.

Voltage regulators perform as desired when regulating from the source to the load and when regulating from a strong source (utility) to a weak source (distributed generation). (See the glossary for definitions of a *strong source* and *weak source*.) Even when the control is provisioned for reverse operation, it has been observed that tap-changing voltage regulators do not perform as desired in reverse when attempting regulation from the weak source to the strong source. The region of performance that is not as well understood is the regulation between sources that are approaching equal strength. As part of this study, we explored all three scenarios: regulator control from a strong source to a weak source (classic case), control from a weak source to a strong source (during reverse power flow), and control between equivalent sources.

In this report, we reassess the topic of existing LTC and line-regulator controls and on a real-world distribution feeder with renewable penetration, and we explore their benefits and disadvantages. This study makes use of metrics such as driving point impedance (DPI), the effectiveness of tap change (tap-delta), reactive power flow, and transformer efficiency to evaluate the performance of LTCs/line regulators on distribution feeders with substantial DER penetrations. These metrics were carefully chosen because they unmask the shortcomings of existing LTC/line regulator control practices on feeders with high DER penetrations. The first chapter takes a deeper dive into the description of these metrics and the reasons we choose them.

This project was executed in three sequential tasks to help the Sacramento Municipal Utility District (SMUD) understand the role of existing LTC/line regulator controllers on distribution feeders with increased DERs. The three tasks of this project are:

- Task 1: Transformer magnetics and thermal characterization
- Task 2: Modeling SMUD distribution system

- Task 3: Use case analysis on a SMUD feeder.

Task 1 comprised the thermal characterization of transformers in the PLECS software modeling and simulation tool. In this task, we modeled a simplified distribution feeder with a wye-wye transformer for line regulators to validate the correlation between the DPI and tap-delta. Additionally, preliminary simulations were run to validate the transformer models. The analysis on this simplified distribution model confirms that the direction of power flow is not a sufficient condition to determine voltage regulation direction in all applications. The details of this task are described in Chapter 1, and Chapter 2 takes a deeper look at this topic on a SMUD feeder.

Task 2 contained preparing a SMUD feeder for a detailed analysis in PLECS. In this task, we converted, reduced, and validated the feeder G011204 from SMUD's territory. The feeder was converted from Synergi to OpenDSS, and the voltages and sequence impedance were compared for validation. The converted feeder contains approximately 4,000 nodes, but PLECS is transient analysis tool and cannot simulate more than 10 three-phase nodes. Hence reduced the feeder from 4,000 nodes to 7 nodes and again compared the reduced feeder to the original Synergi and OpenDSS models.

In Task 3, we used the reduced G011204 feeder validated in Task 2 to assess the impact of DPI on regulator performance. In Chapter 2, we present a model of a distribution feeder from SMUD's territory, and we developed a reduced equivalent in PLECS. The chosen feeder contains a wye-wye configured substation LTC with a delta tertiary. The same feeder also contains a line regulator with open-delta autotransformer configuration. This feeder, with LTC/line regulator, was used to simulate various PV generation levels, and the correlation between local generation and DPI was studied.

The effectiveness of the LTC/line regulator was evaluated using tap-delta, and results confirm that tap-delta varies based on DPI. This study was successful in capturing the LTC/line regulator's tap-delta while the DPI of transformer terminals change as a result of renewable penetration on the selected SMUD distribution feeder. Figure ES-1. captures the tap-delta of the regulator control as the renewable generation increased from 0% to 125% of peak load (5 MW) on a 10-MVA substation. An additional finding was that higher tap-delta's can be obtained by regulating the stronger sources—or, in other words, toward the direction with low DPI. The description of how we arrived at the final result shown in Figure ES-1. is provided in the main text of this report.

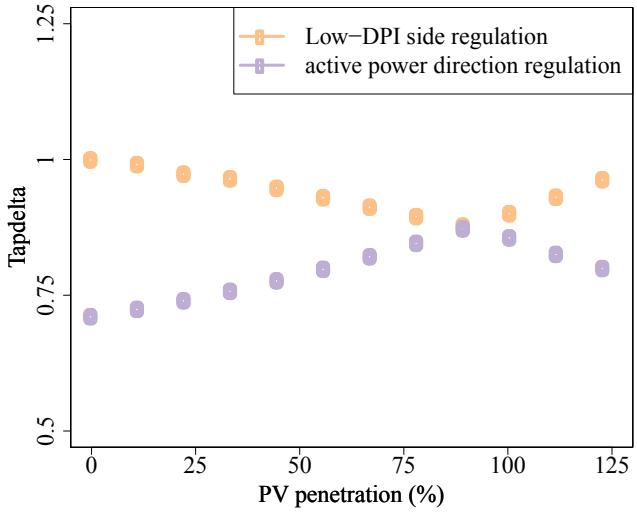

Figure ES-1. Comparison of classic regulator controls (based on power flow direction) to the proposed controls (based on low DPI)

Figure ES-1. shows the tap-delta for two different regulator control methodologies. One trajectory (purple circles) represents tap-delta as the regulator tries to control in the direction of the power flow. Another trajectory (orange circles) represents the tap-delta when a regulator controls in the direction with low DPI. However, the region of performance that is not well understood is the regulation between sources that are approaching equal strength. These results capture the tap-delta when the primary DPI equals the secondary DPI at approximately 90% PV penetration. The tap-deltas have a deflection point around the sources reaching equal strength. The regulator controls have been modeled to be reversible, with Potential Transformers (PT) on both sides of the regulator. That is why we can see the deflection point, whereas no deflection point is shown in Figure 18, even though both scenarios have PV penetrations from 0%–125%. Additionally, the tap-deltas shown in Figure ES-1. are much lower than expected in the field. This is attributed to the transformer models developed in this project. The transformers were modeled with isolation in this effort, whereas in the field there are autotransformers.

In summary, these results point to the effectiveness of line regulators regulating in the direction of low DPI (from the strong source). These results also suggest a number of hypotheses that could be confirmed with future research. For instance, assessing the ease of implementing proposed regulator controls based on DPI on a real feeder needs further research. Also, under tested DPI, impacts on the tap-delta involved only PV generation variations for the peak load day. It could be of interest to capture the impacts of different loading conditions on DPI.

Table of Contents

List of Figures

List of Tables

1 Transformer Magnetics and Thermal Characterization

Increased renewable generation penetration is demanding an update in distribution system voltage control practices as a result of reverse power flow conditions. Although the performance of shunt voltage control equipment (capacitor banks) does not change, series voltage control equipment (voltage regulators and load tap changers [LTCs]) encounters a significant impact from increased distributed energy resources (DERs) [1], [2], [3].

Voltage regulators perform as desired when regulating from the source to the load—i.e., when regulating from a strong source (utility) to a weak source (distributed generation). (See the glossary for definitions of a *strong source* and *weak source*.) Even when the control is provisioned for reverse operation, it has been observed that tap-changing voltage regulators do not perform as desired in reverse when attempting regulation from the weak source to the strong source. The region of performance that is not as well understood is the regulation between sources that are approaching equal strength. As part of this study, we explored all three scenarios: regulator control from a strong source to a weak source (classic case), control from a weak source to a strong source (during reverse power flow), and control between sources that are comparable in strength.

In this task, we modeled and characterized a transformer while operating with existing LTC/line regulator controls. Classic regulator control decided the direction of operation based on the direction of power flow.

Chapter 1 comprises the thermal characterization of the transformer in the PLECS software modeling and simulation tool. In this task, we modeled a simplified distribution feeder with a wye-wye transformer for line regulators to validate the correlation between DPI and tap-delta. Additionally, preliminary simulations were simulated to validate the transformer models. Chapter 2 looks more closely at this topic on a feeder in the Sacramento Municipal Utility District (SMUD).

1.1 Factors to Characterize a Transformer

In this section, we list and describe the factors that are used in the rest of report to evaluate the performance of the LTC/line regulator controls. The following metrics were chosen to characterize the impacts of classic regulator control on transformer life and performance:

- Tap-delta voltage (voltage change per tap) represents the effectiveness of tap-change operation.
- Reactive power flow through the transformer contributed to transformer heating.
- Driving point impedance (DPI) represents the relative strength of the sources (distribution system and DERs).

1.1.1 Factor 1: Tap-Delta

The term *tap-delta* represents voltage change per tap. It is typical that the transformer's taps are adjusted in discrete steps, with each step changing the tap ratio by 0.625% (hence a 10% change requires 16 steps). Because of the varying voltage drops caused by changing loads, LTCs are

often operated to automatically regulate the bus voltage. LTCs/line regulators keep the load's voltage within the specified deadband.

The factor tap-delta represents the effectiveness of regulator operation. The tap-delta has a unit percentage (%) that ranges from 0–100. A value of 100 represents that a step change leads to 100% (0.625%) expected voltage change, whereas a value of 50 represents 50% of expected voltage change. Reduced tap-delta effectiveness leads to higher tap position, thus leading to higher reactive power supply to the load. This is discussed further next, in Section 1.1.2.

1.1.2 Factor 2: Reactive Power Flow through the Transformer

Reactive power flow flows through the transformer to fulfill the load demand. This should not be confused with reactive power losses in the transformer windings. A transformer is a device in which two circuits are coupled by a magnetic field. The mutual flux is the means for energy transfer between the primary and secondary source. This section describes the phenomenon that regulator tap setting decides the quantity of reactive power that flows through the transformer.

The rest of this section discusses the transformer mathematical model to prove the correlation between tap position and reactive power flow in the transformer [4].

Figure 1 presents an equivalent circuit representation of a single-phase transformer.

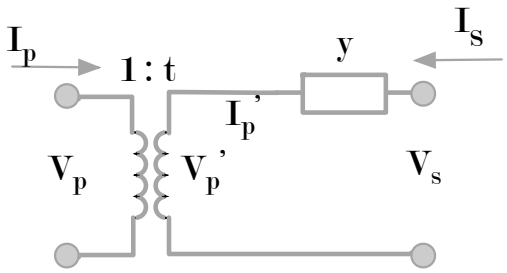

Figure 1. Equivalent circuit for a single-phase transformer with an ideal transformer turns ratio

The voltage and current ratio can be defined as follows:

$$\frac{V_p}{V_s} = \frac{1}{t} \tag{1}$$

$$\frac{I_p}{I_s} = \frac{t}{1} \tag{2}$$

where V_p is the complex voltage at the transformer primary terminal, which is the same as $V_p e^{i\theta_p}$; V_p' is the complex voltage behind the ideal transformer; V_s is the complex voltage at the transformer secondary terminal, which is the same as $V_s e^{i\theta_s}$; and t refers to the tap ratio of the transformer.

The transformer equivalent circuit shown in Figure 1 can be transformed into an equivalent π circuit using the following equations:

$$I_p = tI_s \tag{3}$$

$$I_p = t\left(V_p' - V_s\right)y, \tag{4}$$

$$I_p = t\left(tV_p - V_s\right)y, \tag{5}$$

$$I_p = t^2V_py - tV_sy \tag{6}$$

Similar to the above equation for the transformer primary currents, the equivalent π representation for the transformer secondary current, I_s, is:

$$I_s = tV_py - V_sy \tag{7}$$

From Eq. 6 and Eq. 7, we can generate a matrix form as follows:

$$\begin{bmatrix} I_p \\ I_s \end{bmatrix} = \begin{bmatrix} t^2y & -ty \\ ty & -y \end{bmatrix} \begin{bmatrix} V_p \\ V_s \end{bmatrix} \tag{8}$$

Based on Eq. 8, a comprehensive equivalent π model is shown in Figure 2.

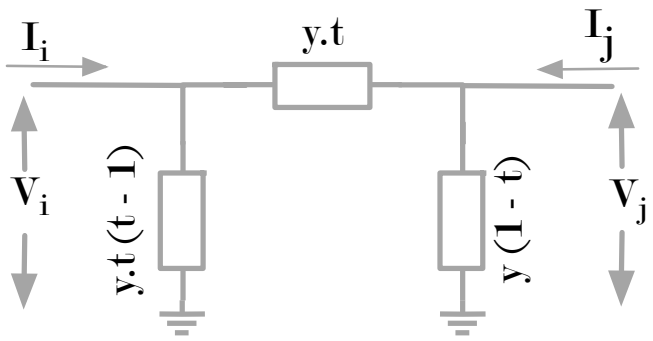

Figure 2. Equivalent π model for the transformer

From Eq. 8, the complex power flows through the transformer can be formulated as:

$$S_{ps} = V_p^*\left[yt(t-1) + \left(V_p - V_s\right)yt\right] \tag{9}$$

$$S_{ps} = V_p^2t^2y - V_p^*V_sty \tag{10}$$

Replacing voltages with phasors—i.e., V_p as $V_pe^{i\theta_p}$ and V_s as $V_se^{i\theta_s}$—and y as $g + jb$ or $y\,e^{j\psi}$ in Eq. 10:

$$S_{ps} = V_p^2t^2(g + jb) - V_pV_sty\,e^{-j(\theta_p - \theta_j - \psi)} \tag{11}$$

In terms of real and reactive power flows:

$$P_{ps} = Re\{S_{ps}\} = V_p^2 t^2 g - V_p V_s t y \cos(\theta_p - \theta_s - \psi) \quad (12)$$

$$Q_{ps} = Im\{S_{ps}\} = V_p^2 t^2 b - V_p V_s t y \sin(\theta_p - \theta_s - \psi) \quad (13)$$

Equation 13 shows that the amount of reactive power flow through the transformer is a function of tap-ratio of the transformer. Transformer operation with a lower tap-delta will lead to an increase in tap position, thus leading to an increase in reactive power flows.

1.1.3 Factor 3: Driving Point Impedance

The DPI is identical with the positive-sequence impedance for static feeder operation conditions. The definition of DPI can be derived from our understanding of strong and weak sources. An ideal strong source—i.e., an infinite bus—is a source of invariable frequency and voltage (both in voltage magnitude and angle) with very high fault currents. The opposite of a strong source is a weak source. Weak sources have sensitive voltages and low fault currents. Higher fault currents occur because strong sources have low DPI. On the contrary, weak sources have high DPI, leading to low fault currents.

The DPI is the equivalent of the sequence impedance that a voltage regulator encounters in real time. The DPI constantly varies, along with the load and photovoltaic (PV) generation on the feeder. Varying renewable generation and loads affect the DPI that a transformer encounters during daily operation. In a typical feeder, as loads increase during peak hours in a day (assuming a fixed load power factor), reactive power demand increases. With the perspective of the regulator, the DPI encountered by the voltage regulator increases. These variations affect the operating conditions of a tap-changing transformer.

The connection between the DPI and reactive power flow is described as follows. In a typical distribution feeder, during peak loads the DPI increases, thus increasing the demand for reactive power. The increase in the reactive power flow through the transformer leads to an increase in voltage drop, thus reducing the tap-delta. A reduced tap-delta with increased DPI can be attributed to the transformer's winding inductance, which is typically 10 to 20 times the resistance of a winding. Hence, an increase in reactive power leads to a voltage drop (caused by the I^2R losses), thus impacting the tap-delta and losses.

The phenomenon of how increased reactive power flow increases losses and reduces output voltage can be better depicted using a phasor diagram, as shown in Figure 3. From the phasor diagram, we can observe that the voltage drops from E1 to V1 and from V2 to E2 are primarily affected by the reactance of the winding. Thus, a further increase in reactive power will lead to an increase in voltage drop.

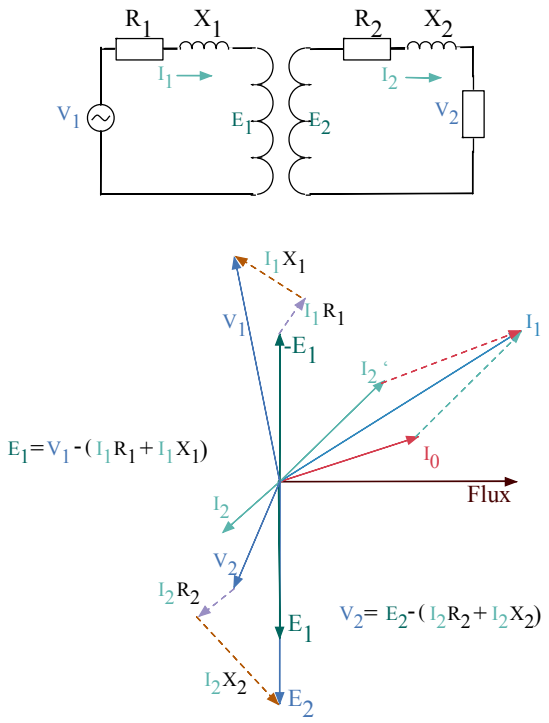

Figure 3. Phasor diagram of a transformer with inductive load depicting the cause for reduced tap-delta voltage during peak load hours

1.1.4 Connection between the Factors and Disambiguation

Typically, substation and line voltage regulators manage distribution system voltage along with other devices, such as shunt capacitors. Classical voltage-regulating devices operate by mechanically changing the transformer's turns ratio by switching taps (increasing or decreasing the number of windings being used). These perform as desired when regulating from the source to the load and when regulating from a strong source to weak source (distributed generation). When the control is provisioned for reverse operation, it has been observed that tap-changing voltage regulators do not perform as desired when attempting regulation from the weak source to the strong source. They actually perform predictably backward, and they end up regulating the weak source. The region of performance that is not as well understood is the regulation between sources that are approaching equal strength.

Decades ago, it was determined that the effectiveness of a tap change declines as the strength of the sources become similar. For a source strength ratio of 10:1 (or 1:10), a tap change of 2% of the windings should produce a 2% change in voltage. But as this ratio approaches 1:1, a 2% tap change produces a voltage change less than 0.5%. In addition to impacting the effectiveness of voltage regulation, this situation can produce detrimental heating in the equipment windings for sources with relatively equivalent strengths.

To summarize, the DPI that the device encounters decides the magnitude and phase of the current that flows out of a device. This DPI sets the current and the power factor of the current that enters or leaves a transformer winding. Higher DPI can lead to increased reactive power flow, thus reducing tap-delta.

A common understanding is that DPI is similar to fault duty. A typical utility practice is to calculate the DPI is by calculating the fault current while measuring the voltage. This practice works well in traditional feeders without DERs. In traditional feeders, loads are mostly passive and do not contribute much to fault currents; however, DERs contribute to fault currents.

In transmission system studies, because of the higher voltage levels of operation, renewable resources are modeled as current sources. Hence, the impact on fault duty from these renewable resources is neglected. Increasingly, in distribution feeders this assumption is not valid because at the distribution voltage the fault level contribution by DER is no longer negligible.

With increasing amounts of DERs, fault duty does not represent DPI exactly. Task 2 of this study looked into this issue. Additionally, the sensitivity of DPIs with increasing PV penetration levels was studied.

1.2 Transformer Characterization

This section presents the details pertaining to the models developed in this project to characterize transformer magnetics. This study develops a transformer model in a transient analysis tool, PLECS, to ensure realistic modeling. As a part of the development, magnetic modeling is performed [5].

1.2.1 Modeling Effort

Compared to other passive components, transformers with magnetic components are rather difficult to model for the following reasons:

- Transformers, especially those with multiple windings, can have complex geometric structures. The flux in the magnetic core might be split into several paths with different magnetic properties. In addition to the core flux, each winding has its own leakage flux.
- Core materials such as iron alloy and ferrite express a highly nonlinear behavior. At high flux densities, the core material saturates, leading to reduced inductive impedance. Moreover, hysteresis effects and eddy currents cause frequency-dependent losses. In PLECS, the user can build complex magnetic components in a special magnetic circuit domain. Core functionalities—such as windings, cores, and air gaps—are provided in the Magnetics Library. The available core models include saturation and hysteresis. Frequency-dependent losses can be modeled with magnetic resistances. Windings form the interface between the electrical and the magnetic domain. Alternatively, less complex magnetic components, such as saturable inductors and single-phase transformers, can be modeled directly in the electrical domain.

1.2.1.1 Conventional Transformer Modeling

In the coupled inductor approach, the magnetic component is modeled directly in the electrical domain as an equivalent circuit in which the inductances represent magnetic flux paths and losses incurred at the resistors. Magnetic coupling between windings is realized with either mutual inductances or ideal transformers.

Using coupled inductors, magnetic components can be implemented in any circuit simulator because only electrical components are required. This approach is most commonly used to

represent standard magnetic components, such as transformers. Figure 4 shows an example for a two-winding transformer, where Lσ1 and Lσ2 represent the leakage inductances, Lm represents the nonlinear magnetization inductance, and Rfe represents the iron losses. The copper resistances of the windings are modeled with R1 and R2.

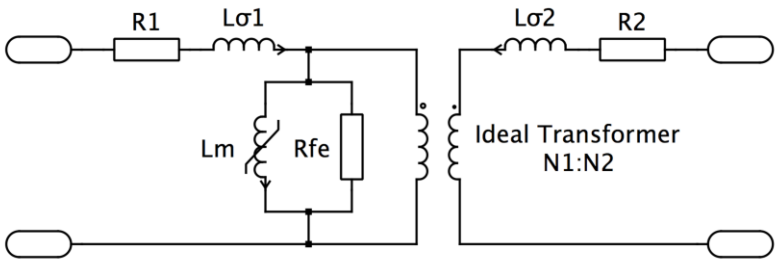

Figure 4. Transformer implementation with coupled inductors

However, the equivalent circuit bears little resemblance to the physical structure of the magnetic component. For example, parallel flux paths in the magnetic structure are modeled with series inductances in the equivalent circuit. For nontrivial magnetic components, such as multiple-winding transformers or integrated magnetic components, the equivalent circuit can be difficult to derive and understand. In addition, equivalent circuits based on inductors are impossible to derive for nonplanar magnetic components.

1.2.1.2 Magnetics Domain Modeling in PLECS

The magnetics domain provided in PLECS is based on the permeance-capacitance analogy. The magnetic library comprises windings, constant and variable permeances, as well as magnetic resistors. By connecting them according to the physical structure, the user can create equivalent circuits for arbitrary magnetic components. The two-winding transformer shown in Figure 4 will look like the schematic shown in Figure 5 when modeled in the magnetic domain.

Pσ1 and Pσ2 represent the permeances of the leakage flux path, Pm the nonlinear permeance of the core, and Gfe dissipates the iron losses. The winding resistances R1 and R2 are modeled in the electrical domain.

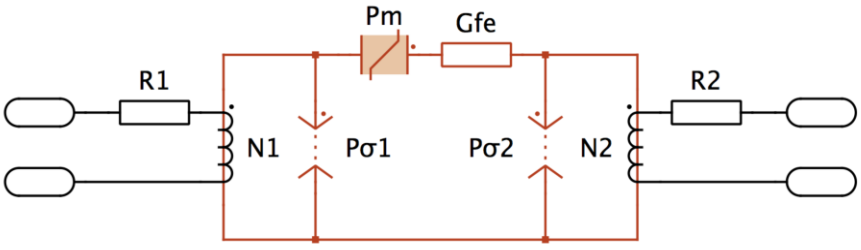

Figure 5. Transformer implementation in the magnetic domain

1.3 Results and Discussions

The factors described in Section 1.1 (tap-delta and reactive power flow through the transformer) will be quantified and analyzed in this section for various system conditions. A one-line diagram

of the test system is shown in Figure 6. This system represents a simplified distribution system with a voltage regulator situated halfway from the feeder substation. This system ignores the many lines from each bus to multiple other buses as well as numerous renewable resources and loads present on the system; however, this test system highlights the complexities of the overall distribution system and many factors that need to be included in the analysis, such as the changes that occur during system operation [1]. The test system for analysis was built in PLECS. This section quantifies what happens inside a transformer for varying distribution system conditions, such as DPI ratios and power factors.

The thermal component will be characterized using reactive power flow in a transformer. Losses inside the transformer are characterized using efficiency. The transient analysis tool, PLECS, will be used for device characterization. Magnetics, reactive power flows, and tap-delta voltage for varying values of DPI will be calculated. A model as shown in Figure 6 is developed in PLECS to help analyze the impacts of DPI and power factor on transformer operation.

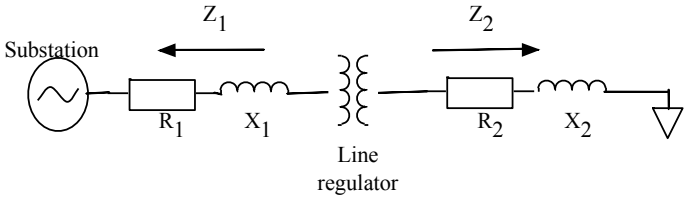

Figure 6. One-line diagram of the simplified distribution system developed in PLECS

For the simplified model shown in Figure 6, a transformer with wye-wye configuration is used. The purpose behind these initial runs on a simplified model is to validate the impact of DPI on tap-delta. This study performs three use cases:

1. Vary the DPI ratio (vary Z2 with Z1 constant, thus varying the Z2-to-Z1 ratio), and capture the secondary tap-delta, reactive power flow, and efficiency.
2. Vary the DPI ratio (Z2/Z1), and capture the primary and secondary tap-delta.
3. Vary the DPI ratio (Z2/Z1), and capture the primary and secondary tap-deltas for different loading conditions.

The analysis of these extreme cases (any of which could automatically occur in varying degrees as a result of system switching) suggests the possibility that the direction of power flow might not be an appropriate condition to determine the voltage regulation direction in all applications.

Because existing regulator/LTC control algorithms can switch the direction of regulation based on the direction of power flow, the regulator can attempt to regulate the side with higher DPI (Z2), where (Z2/Z1 > 1).

Z1 and Z2 represent the DPI as shown in a real distribution feeder on the primary (upstream/substation) and secondary (downstream) terminal of a transformer, respectively. This study considers a scenario of a line regulator situated halfway from the substation. A DPI ratio less than 1 represents a scenario in which the primary DPI is higher than the secondary DPI, which can be caused when there is excessive reverse power flow. A DPI ratio more than 1

represents a scenario in which the secondary DPI is higher than the primary DPI, which can be caused during low PV penetration scenarios. The DPI is decided by the stiffness of the feeder.

1.3.1 Core Losses and Efficiency in a Transformer

Figure 7 shows the core losses and efficiency for varying DPI (Z2/Z1) ratios. DPI Z2 is varied while keeping Z1 constant, thus changing the ratio between Z2 and Z1. The DPI ratio Z2/Z1 is varied from 0.2 to 10 while core losses and efficiency is captured in the PLECS model. A DPI ratio less than 1 represents a scenario in which the primary DPI is higher than the secondary DPI, which can be caused when there is excessive reverse power flow.

For different DPI scenarios, flux in the core is practically constant. The load component current always neutralizes the changes in the load. The PLECS model showed that flux in the core is practically a constant.

The transformer efficiency is characterized in Figure 7. For increasing DPI ratios, the efficiency reduces. Overall, an efficiency drop of 1% is observed when the DPI ratio increases from 0.2 to 10. Higher DPI ratios lead to increased reactive power demand, thus leading to increased losses. The results are coherent with conventional understanding. These two results depict the accuracy of the magnetic domain model in PLECS.

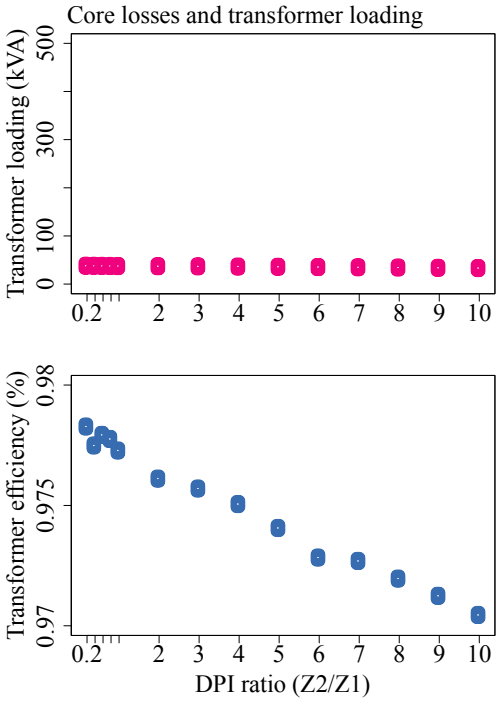

Figure 7. Magneto-motive force and core losses as the impedance ratio of Z2/Z1 changes

1.3.2 Secondary Winding Tap-Delta and Reactive Power Transferred in a Transformer for Changing Impedance Ratios

Figure 8 shows the impact on transformer secondary tap-delta (voltage change per tap change) and reactive power supply to load as the ratio of primary to secondary DPI (Z2 to Z1) presented in Figure 9 is varied. The increase in the DPI ratio from 0.2 to 10 leads to a significant increase in the reactive power flow and a drop in tap-delta. A DPI ratio less than 1 represents a scenario in which the primary DPI is higher than the secondary DPI, which can be caused when there is excessive reverse power flow.

The reactive power to load through the transformer increased tenfold as the DPI ratio was increased from 1 to 10. The tap-delta voltage dropped from 0.94to 0.66 as the DPI ratio was increased from 0.2 to 10.

In an ideal scenario, the expected voltage change per-tap was 1, whereas for a DPI ratio of 10 (Z2 is 10 times Z1), the voltage change per-tap was observed to be 0.7. In this situation, the regulator control will raise steps until the terminal voltage reaches the deadband. This scenario will lead to a further increase in the reactive power transferred across the transformer. For a DPI ratio (Z2/Z1) of 10 (Z2 is 10 times the DPI Z1), a 1% turns ratio change raised the voltage at the secondary terminal by only 0.6%. The internal transformer voltage drop negated 0.4% of the turns ratio change. Controlling the transformer terminal with high DPI is more effective for volt-ampere reactive control than voltage control.

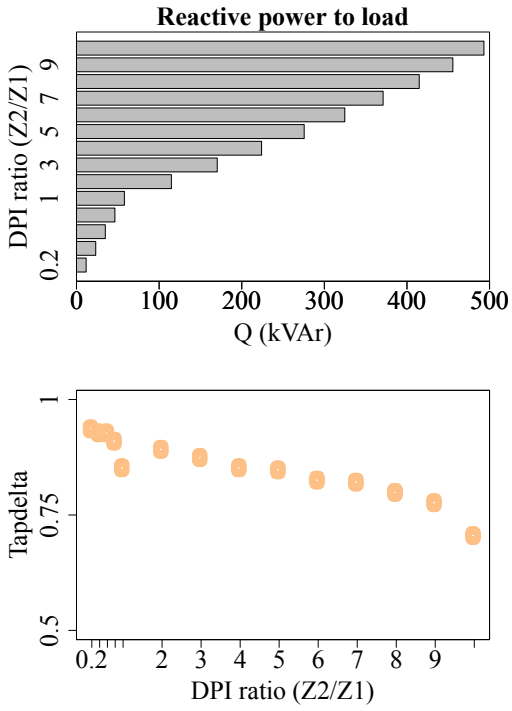

Figure 8. Transferred reactive power and tap-delta voltage for varying DPI ratios

1.3.3 Secondary Winding and Primary Winding Tap-Delta Measurements at Transformer Primary and Secondary Terminal with Classic Secondary Winding Controls

A regulator control fulfills the varying reactive power requirement by changing the taps, typically at the secondary transformer windings, by either stepping up or down the secondary winding taps. In the process of increasing or decreasing the secondary voltage, the primary voltage drops caused by increased losses that result from an increased reactive component in the line currents. This phenomenon is captured while simulating the extreme cases of DPI ratios on the simplified distribution system presented in Figure 6. The DPI ratios for Z2 to Z1, with reference to Figure 6, were varied from 0.1 to 12. For a DPI ratio of 1, Z2 equals Z1; whereas for DPI ratio of less than 1, Z1 is more than Z2, and vice versa. A DPI ratio less than 1 represents the scenario in which a strong source is controlling the weak source. A DPI ratio more than 1 represents a situation in which a load side is controlling the substation side.

As DPI ratios were varied from 0.1 to 12, the load was set to a 1.5 MW with 0.95 power factor, and the regulator tap setting was set to 5. It was considered that the regulator controls change the secondary taps. Figure 9 presents the tap-delta—i.e., the effectiveness of tap change operation—at the primary and secondary transformer windings for varying DPI ratios.

Figure 9 contains two components: the left bar plot represents the primary winding tap-delta, and the right bar plot represents the secondary winding tap-delta. The x-axis represents the tap-delta ranges from -1 to +1. A value of 1 represents that a tap change operation was 100% effective. Figure 9 shows that as the regulator control tries to control the secondary winding, the primary winding encounters a drop in voltage caused by increased losses.

In an ideal transformer (without losses), the red bar and blue bar are expected to add up to unity; however, the results in Figure 9 do not add up to unity. The missing component is the losses that occur in the transformer windings. The load losses are likely exaggerated because of the transformer models developed in this project. The transformers were modeled with isolation in this effort, whereas in the field there are autotransformers.

Figure 9 captures the primary and secondary tap-delta as system operating conditions vary.

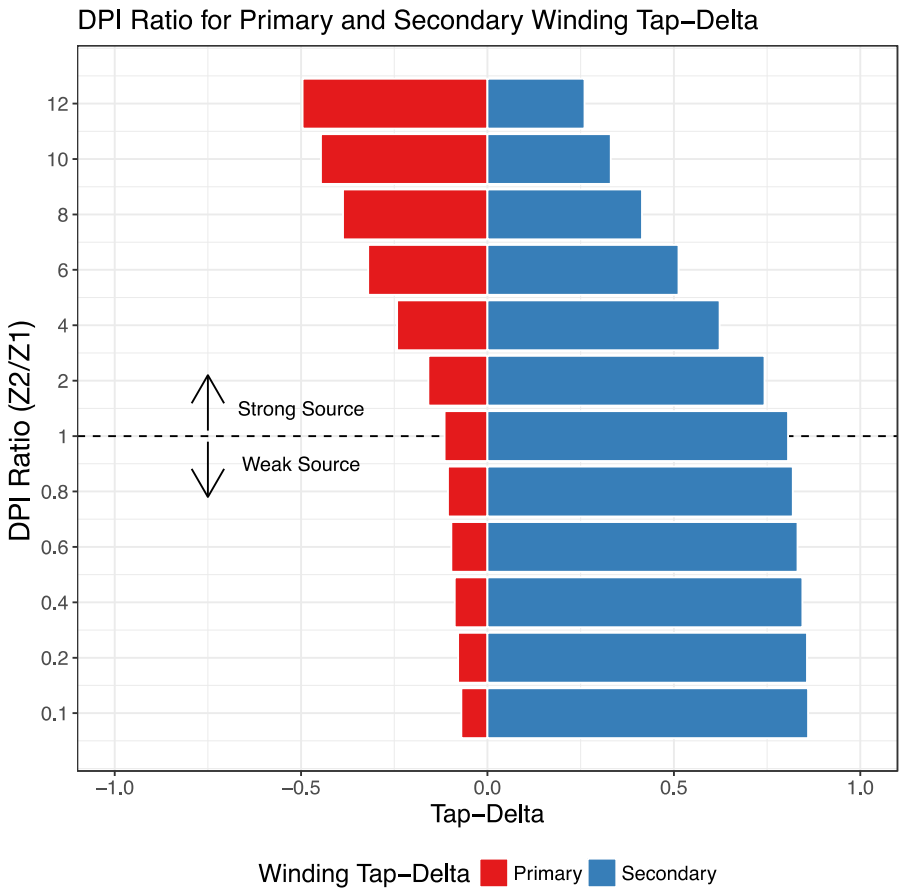

Figure 9. Primary and secondary tap-delta for varying DPI ratios with fixed load and tap setting

The summary from Figure 9 is as follows:

- Voltage regulators perform as desired when regulating from the source to the load and when regulating from a strong source to a weak source (distributed generation).
- When the control is provisioned for reverse operation, it has been observed that tap-changing voltage regulators do not perform as desired when attempting regulation from the weak source to the strong source.
- As the regulator tries to regulate the weaker source (high DPI), the secondary winding tap-delta reduces, and the primary winding voltage drop increases.
- The secondary winding tap-delta reduces from 0.9 to 0.3 as the DPI ratio of Z2/Z1 increases from 0.1 to 12. The ideal expected tap-delta is 1; whereas for a DPI ratio of 12, only a 0.3 tap-delta occurs.
- The primary winding tap-delta decreases (negative tap-delta) from 0 to -0.5 for increasing DPI ratios. Because of increased currents, the losses at the primary winding increase, thus causing a higher voltage drop

As a part of this study, we explored all three scenarios: regulator control from a strong source to a weak source (classic case), control from a weak source to a strong source (during reverse power flow), and controlling sources that are equivalent.

1.3.4 Secondary Tap-Delta Measurements at Transformer with Both Primary and Secondary Winding Controls

Ideally, regulator controller almost always regulates the secondary winding of the transformer. In this study, primary winding refers to the substation side, and secondary winding refers to the load side; however, this section considers a scenario in which the regulator controller has a choice between the primary and secondary winding. Additionally, this section considers a possibility in which the regulator controller can identify and regulate the low DPI side for all extreme cases.

As the DPI ratios were varied from 0.1 to 9, the loads were set to 1.5 MW, 3 MW, and 4.5 MW at 0.95 power factor, and the regulator tap setting was set to 5. It was considered that the regulator controls can change the primary and secondary winding taps. Figure 10 presents the tap-delta—i.e., the effectiveness of tap change operation—at the primary and secondary transformer windings for varying DPI ratios.

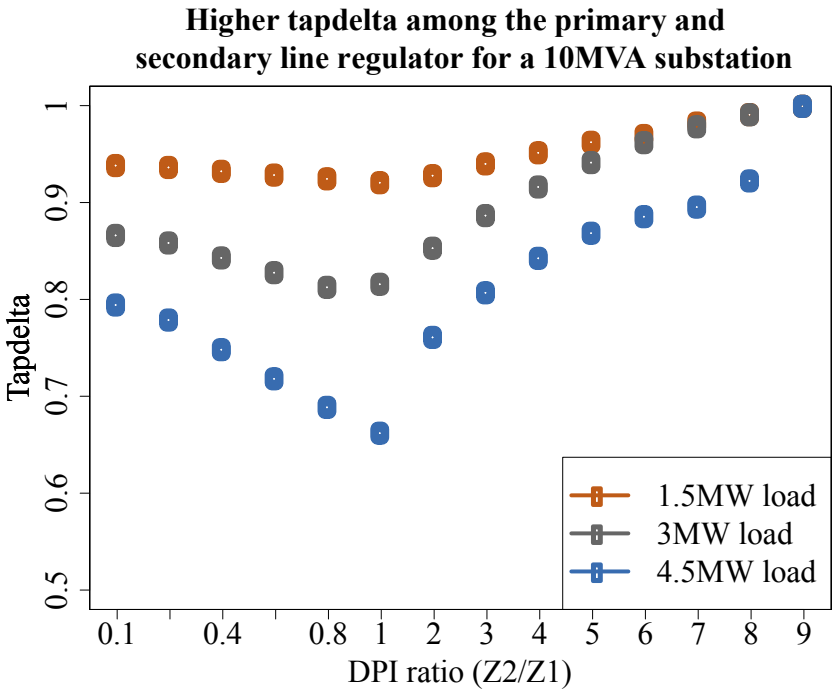

Figure 10. Higher tap-delta among the primary and secondary transformer windings with an assumption that the regulator controller can regulate primary or secondary windings with low DPI

Figure 10 presents the tap-delta for a regulator controller that chooses to control the winding with low DPI. The DPI ratios were varied from 0.1 to 9, and the tap-deltas were captured. Results in Figure 10 can be categorized into three scenarios: for a DPI ratio less than 1, Z1 will be higher than Z2; for a DPI ratio of 1, Z1 equals Z2; and for a DPI ratio more than 1, Z2 is more than Z1.

- DPI ratio less than 1: For this scenario, Figure 10 shows that the tap-delta decreases as the DPI ratio increases from 0.1 to 0.9. The regulator controls the secondary winding, which is a typical practice. Because the DPI on the primary transformer winding is more than transformer secondary winding, the regulator chose to control the transformer secondary terminal.
- DPI ratio equal to 1: For this scenario, the DPIs that a transformer encounters on both sides are equal. Hence the effect of tap change operation on primary or secondary winding is identical.
- DPI ratio more than 1: This particular scenario is when Z2 is more than Z1 (Figure 6). The regulator control chooses to control the primary winding because Z1 is less than Z2. As Z2 continues to increase, the DPI-based regulator control achieves a higher tap-delta.

2 Use Case Analysis on SMUD Feeder

In this chapter, we discuss the effects of DPI on regulator performance on a real SMUD feeder. In Chapter 1, we presented a model of a distribution feeder from SMUD territory and developed a reduced equivalent in PLECS. The substation LTC was modeled as a wye-wye configured substation LTC with delta tertiary. The same feeder also contains a line regulator with open-delta autotransformer configuration. This feeder with LTC and line regulator were simulated for various PV generation levels, and the effects of DPI were studied on regulator performance. Details of LTC and line regulator configurations are presented in the following sections.

2.1 Transformer Model Description

The SMUD distribution feeder G011204 was reduced and modeled in PLECS. We added a substation LTC and a line regulator to the validated PLECS model, as shown in Figure 11. A wye-wye three-phase transformer with delta tertiary was modeled for the substation bank, whereas an open-delta autotransformer was modeled for the line regulator. Both devices (LTC and line regulator) were modeled with a tap-changing under-load controller in PLECS. The tap-changing under-load controller model in PLECS can take the tap position as an input to set the voltage on either the secondary or primary transformer winding. Descriptions of the developed LTC and line regulator transformer models are provided next.

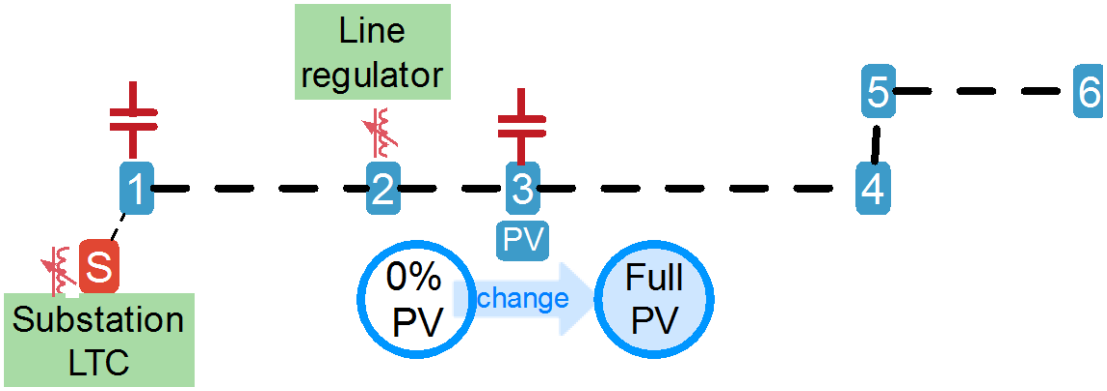

Figure 11. View of the reduced feeder with substation LTC and line regulator included

2.1.1 Wye-Wye Connection with Delta Tertiary

For the chosen feeder, G011204, the LTC was modeled using a wye-wye with delta tertiary connections. This connection is ordinarily used to accommodate single-phase loads and three-phase loads. When a voltage is transformed from primary to secondary, the voltage waveform in the primary winding gets distorted. This distorted wave comprises the original 60-Hz sine wave along with a series of harmonics containing three times the original, five times the original, etc. These harmonics in the sine wave can flow to the ground through neutral when connected in wye, or in delta connection these fluctuations circulate around the connection producing little heat. This is a simplified explanation of the phenomenon.

Particularly for a wye-connected winding without a return-to-ground, the harmonics are bothersome. To overcome this, some wye-connected transformers are provided with small-capacity auxiliary windings connected in delta, as shown in Figure 12.

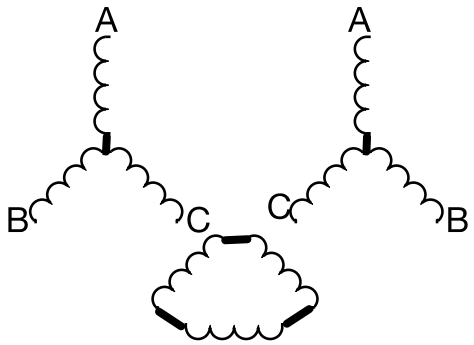

Figure 12. Winding diagram for a three-phase wye-wye transformer with delta tertiary

2.1.2 Open-Delta Transformer

For the chosen feeder, G011204, the line regulator was modeled using an open-delta autotransformer and LTC as a wye-wye with delta-tertiary connections. The line-regulator as an autotransformer might be viewed as a particular type of transformer whose characteristics make it more advantageous for certain conditions. An autotransformer has only one winding, a portion of which serves both as the primary and secondary windings. In this type of transformer, only a portion of electrical energy is transformed, and the remainder flows conductively through its windings; whereas in a two-winding transformer, all the energy is transformed. Hence autotransformers have a smaller footprint than the equivalent two-winding transformer. Figure 13 presents a single-line diagram of an open-delta transformer shared by SMUD, and it was used to generate the transformer model in PLECS. The open-delta configuration consists of two autotransformers connected line-to-line between phases A-B and phases B-C. Each of two autotransformers are controlled independently using regulator controls.

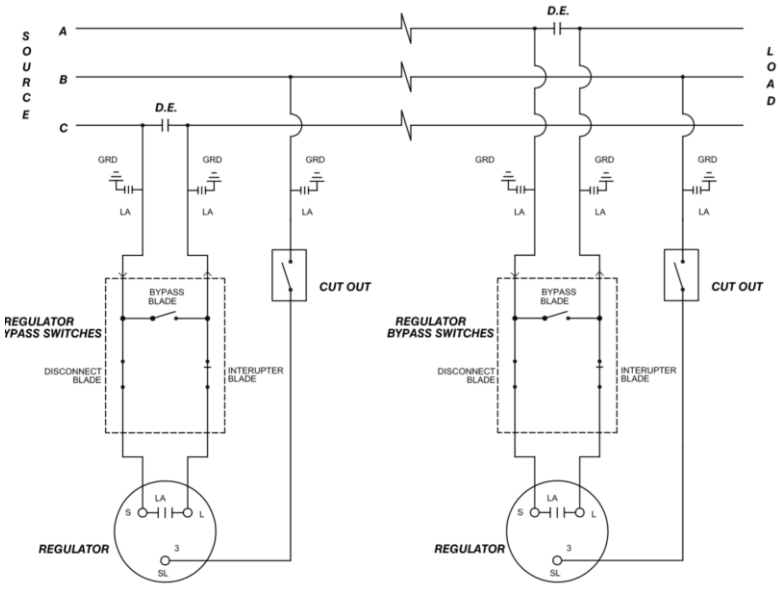

Figure 13. Single-line diagram of an open-delta configuration used in the chosen SMUD feeder's line regulators

2.2 Results and Discussions

This section provides a detailed discussion on the two use cases simulated in this task and the respective results:

- Case 1: Substation LTC. In Case 1, the effects of DPI on substation LTC are explored.
- Case 2: Line regulator. In Case 2, the effects of DPI on line regulator are explored

The following sections present the reactive power transfer, tap-delta, transformer efficiency, and transformer core losses for these two use cases. The above-mentioned factors were captured for varying PV penetration levels for both use cases. Additionally, the tap-deltas were compared when controlling the high DPI side (weak source) and low DPI side (strong source) for the line regulator operations. We ran the peak day with varying PV conditions to capture these factors.

The PV generator was modeled as a PQ resource—in other words, as a current source. The PV generator penetration is calculated as a percentage of the peak load.

2.2.1 Use Case 1: Substation LTC

In this section, we present the results capturing the effects of varying PV generation conditions on substation LTC operation. The reduced feeder with a wye-wye configured substation LTC under simulation for Case 1 is shown in Figure 14. In this case, the PV penetration was varied from 0% to 125% while the LTC metrics—such as reactive power transfer, tap-delta, transformer efficiency, and transformer core losses—were captured.

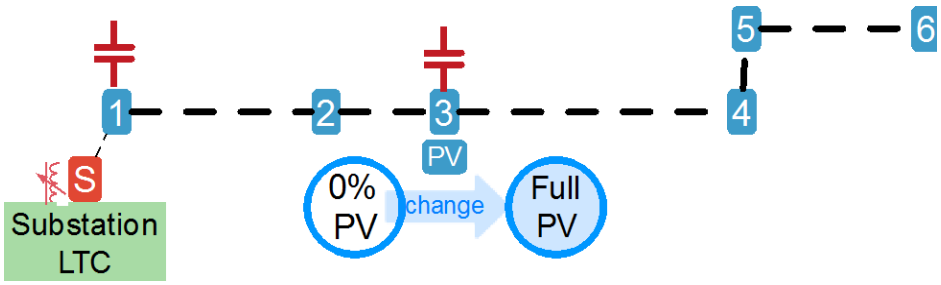

Figure 14. Reduced feeder model with substation LTC for Case 1

Figure 15 shows the impact of varying PV penetration on tap-delta (voltage change per tap change) and reactive power supply to load. The increase in PV penetration from 0% to 125% led to a significant increase in the reactive power flow and tap-delta. PV penetrations more than 80% represent a scenario when there was excessive reverse power flow.

The reactive power to load through the transformer increased as PV penetration increased from 0% to 100%. The increase in PV penetration led to a drop in DPI, thus affecting the tap-delta as well. The tap-delta increased from 0.65 to 1 as the DPI increased because of the PV penetration.

The expected voltage change per tap was 1; whereas for PV penetration of 0%, the voltage change per tap was observed to be 0.65. In this situation, the automated regulator control will raise the transformer taps until the sensed voltage falls within the regulator control deadband (typically 3 V). A raised tap setting will lead to a further increase in the reactive power

transferred across the transformer. For PV penetration of 125%, a tap-delta of 1 was observed. This result confirms that PV penetration affects the DPI and hence tap-delta.

Figure 16 presents the transformer core losses and efficiency for varying levels of PV penetration. Transformer core losses reduced, leading to increased efficiency as PV penetration levels increased from 0% to 125%. This result represents the correlation between PV penetration levels and transformer performance. Increased PV penetration reduced the substation load, thus leading to reduced DPI. As the DPI reduced with increasing PV penetration, the tap-delta increased.

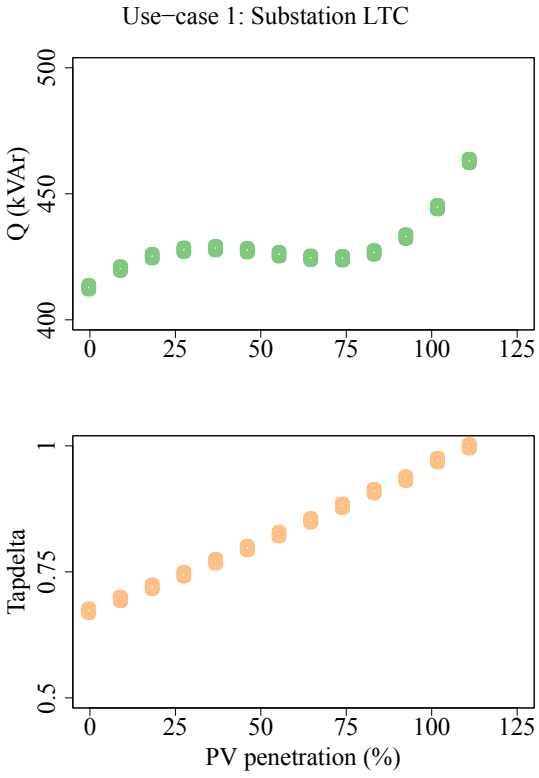

Figure 15. Tap-delta and reactive power transfer for varying PV penetration levels in Case 1

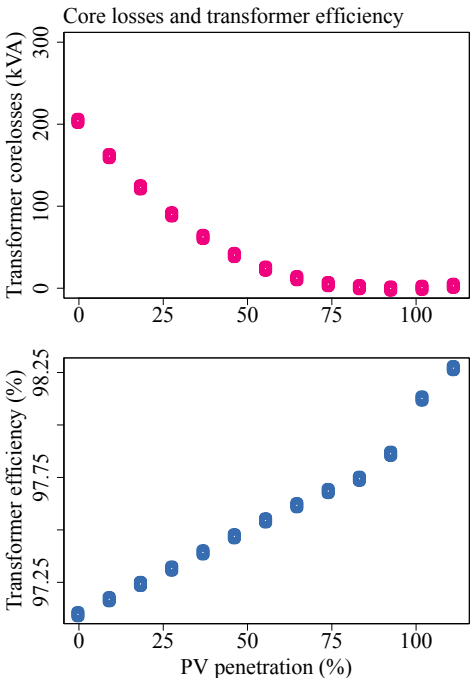

Figure 16. Transformer efficiency and core losses for varying PV penetration levels in Case 1

2.2.2 Use Case 2: Line Regulator

In this section, we present the results capturing the effects of varying PV penetration conditions on line regulator operation. Figure 17 shows the reduced feeder with an open-delta-configured line regulator under simulation for Case 2. In this case, PV penetration was varied from 0% to 125% while the line regulator metrics—such as reactive power transfer, tap-delta, transformer efficiency, and transformer core losses—are captured.

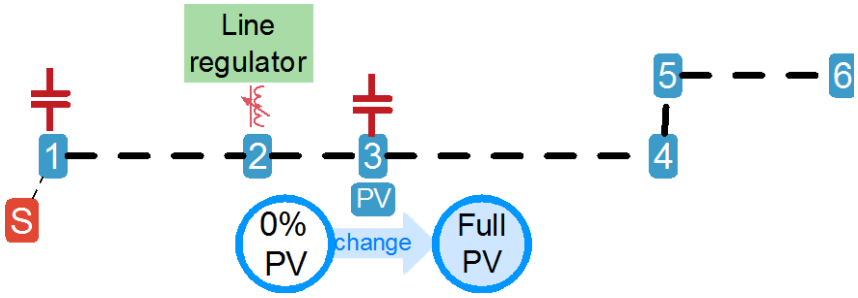

Figure 17. Reduced feeder model with line regulator for Case 2

Figure 18 shows the impact of varying PV penetration on tap-delta (voltage change per tap change for line regulator) and reactive power supply to load. In this model, the regulator controls were modeled with the ability only to vary the secondary winding tap. The increase in PV penetration from 0% to 100% led to an increase in reactive power flow and tap-delta. PV penetration more than 80% represents a scenario when there is reverse power flow.

The reactive power to load through the transformer increased as PV penetration increased from 0% to 100%. An increase in PV penetration led to a drop in DPI, thus affecting the tap-delta as well. The tap-delta increased from 0.7 to 0.95 as the DPI increased as a result of PV penetration.

The expected voltage change per tap was 1; whereas for PV penetration of 0%, voltage change per tap was observed to be 0.65. In this situation, the automated regulator control will raise the regulator taps until the sensed voltage falls within the regulator control deadband (typically 3 V). A raised tap setting will lead to a further increase in the reactive power transferred across the transformer. For PV penetration of 125%, a tap-delta of 0.95 was observed. This result confirms that PV penetration affects the DPI and hence tap-delta.

Figure 19 presents the transformer core losses and efficiency for varying levels of PV penetration. Transformer core losses reduced, leading to increased efficiency as PV penetration levels increased from 0% to 125%. This result represents the correlation between PV penetration levels and transformer performance. Increased PV penetration reduced the substation load, thus leading to reduced DPI. As the DPI reduced with increasing PV penetration, the tap-delta increased.

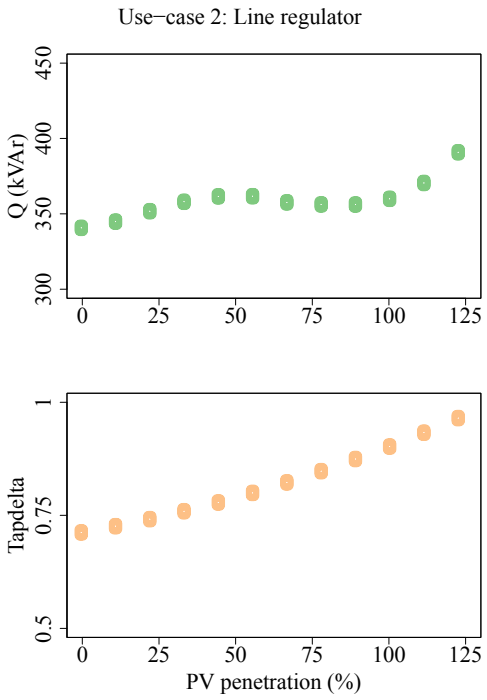

Figure 18. Tap-delta and reactive power transfer for varying PV penetration levels in Case 2

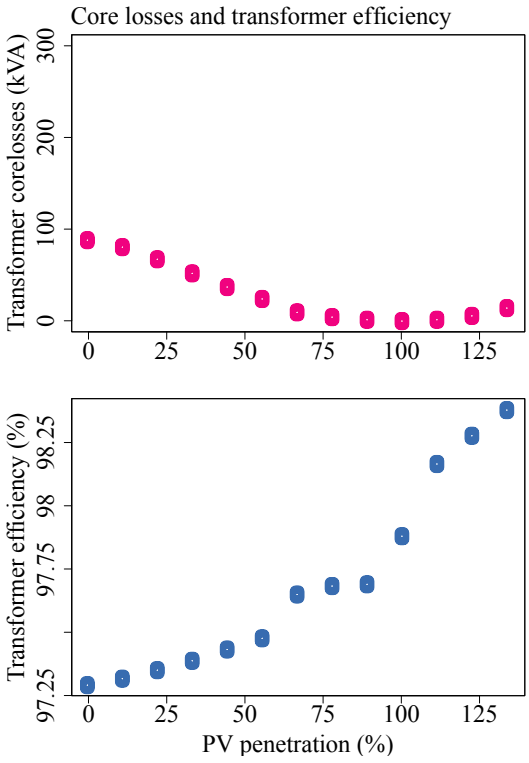

Figure 19. Transformer efficiency and core losses for varying PV penetration levels in Case 2

2.2.3 Regulator Control Direction Based on the Low DPI Side

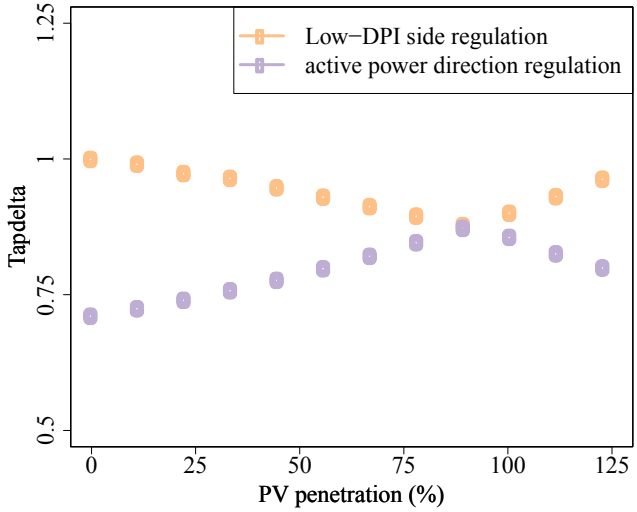

Figure 20. Comparison of classic regulator controls (based on power flow direction) to the proposed controls (based on low DPI)

Figure 20 shows the tap-delta for two different regulator-control methodologies. One trajectory (purple circles) represents the tap-delta as the regulator tries to control in the direction of power flow. Another trajectory (orange circles) represents the tap-delta when the regulator controls in the direction with low DPI. The regulator controls have been modeled to be reversible, with PT's on both sides of the regulator. That is why we can see the deflection point, whereas no deflection point is shown in Figure A-8, even though both scenarios have PV penetrations from 0%–125%. Additionally, the tap-delta's that are shown in Figure ES-1. are much lower than expected in the field. This is attributed to the transformer models developed in this project. The transformers were modeled with isolation in this effort, whereas in the field there are autotransformers.

As mentioned in Chapter 1, the region of performance not well understood is the regulation between sources that are approaching equal strength. These results capture the tap-delta when the primary DPI equals the secondary DPI when PV penetration levels are approximately 90%. The tap-deltas have a deflection point around the sources reaching equal strength.

Figure 20 shows the results of the strong source controlling the weak source, sources with equal strength, and the weak source controlling the strong source. For PV penetration levels up to 90%, the direction of power flow is from the substation to the load. At approximately 90% PV penetration, the DPIs on the primary and secondary side of the regulator are similar; however, for PV penetration levels more than 90%, the DER side will control the substation side.

For the chosen SMUD feeder's peak loading condition (5 MW), reverse power flow is observed for 90% PV penetration levels because of the location of the DER. For PV penetration levels up to 90%, regulating the primary side of the transformer yielded an increased tap-delta. Figure 20 shows that for 90% PV penetration (self-supply scenario), regulating the primary taps yields the same tap-delta as regulating the secondary taps.

As evident by the orange circles, for PV penetration levels more than 90%, regulating the transformer on the secondary side yielded an increased tap-delta. Thus, regulating the direction based on low DPI always yields a higher tap-delta when compared to existing controls.

Discussions and Conclusions

Increased renewable penetration is demanding an update in distribution system voltage control practices caused by reverse power flow conditions. Although shunt voltage control equipment (capacitor banks) does not see any change, series voltage control equipment (voltage regulators, LTCs) encounters a significant impact from increased DERs.

In this report, we researched the topic of existing LTC/line regulator controls and their disadvantages on a distribution feeder with high DER penetrations. Voltage regulators perform as desired when regulating from the source to the load and when regulating from a strong source to a weak source (distributed generation). When the control is provisioned for reverse operation, it has been observed that tap-changing voltage regulators do not perform as desired when attempting regulation from the weak source to the strong source. The region of performance that is not as well understood is regulation between sources that are approaching equal strength. As part of this study, we explored all three scenarios: regulator control from the strong source to the weak source (classic case), control from the weak source to the strong source (during reverse power flow), and control between sources that are equivalent.

This study made use of metrics such as DPI, effectiveness of tap change (tap-delta), reactive power flow, and transformer efficiency to evaluate the performance of LTCs/line regulators on distribution feeders with substantial DER penetration. These metrics were carefully chosen because they unmask the shortcomings of existing LTC/line regulator control practices on high DER penetration feeders.

The project was executed under three tasks. Task 1 comprised the thermal characterization of the transformer in the PLECS software modeling and simulation tool. In this task, we also modeled a simplified distribution feeder with a wye-wye transformer for line regulators to validate the correlation between DPI and tap-delta. Voltage regulator performance was categorized under three conditions:

- Regulating from the source to the load—i.e., when regulating from a strong source to a weak source (distributed generation).
- Regulation from the weak source to the strong source.
- Regulation between sources that are approaching equal strength.

As a part of this study, we explored all three scenarios: regulator control from the strong source to the weak source (classic case), control from the weak source to the strong source (during reverse power flow), and control between sources that are equivalent.

Task 2 involved preparing SMUD's feeder for a detailed analysis in PLECS. In this task, we converted, reduced, and validated the feeder G011204 from SMUD's territory. The feeder was converted from Synergi to OpenDSS, and the voltages and sequence impedance were compared for validation. The converted feeder contained approximately 4,000 nodes, but PLECS is a transient analysis tool and cannot simulate more than 10 three-phase nodes. Hence, we reduced the feeder from 4,000 nodes to 7 nodes, and again we compared the reduced feeder to the original Synergi and OpenDSS models. In Task 3, we used the reduced G011204 feeder validated in Task 2 to assess the impact of DPI on regulator performance. The chosen feeder

contained a wye-wye configured substation LTC with delta tertiary. The same feeder also contained a line regulator with open-delta autotransformer configuration. This feeder with LTC and line regulator was simulated for various PV generation levels, and the correlation between local generation and DPI was studied.

The effectiveness of LTC/line regulator was assessed using tap-delta, and the results confirmed that tap-delta varies based on DPI and that DER penetration affects the DPI of distribution feeders. The key finding of the report is presented in Figure 20. The summary of findings is that regulator performance can be studied under three operation conditions. The three parts are strong source controlling the weak source, sources with equal strength, and weak source controlling the strong source. Varying amounts of PV penetrations were modeled to evaluate the regulator performance.

For the analysis, we used a SMUD distribution feeder with 5-MW peak load at 0.95 power factor on a 10-MVA substation and with 3 MW of PV generation halfway down the feeder. For PV penetration levels up to 90% (ratio of peak load), the direction of power flow is from the substation to the load—i.e., the strong source controlling the weak source. At approximately 90% PV penetration, the DPIs on the primary and secondary of the regulator are similar; however, for PV penetration levels more than 90%, reverse power flow can be observed.

Results (Figure 20) confirmed our initial understanding that higher tap-delta's could be obtained by regulating from stronger sources or from the direction with low DPI. In summary, these results point to the effectiveness of regulating line regulators from the direction of low DPI. Figure 20 shows that deciding the direction of regulation based on DPI is always efficient compared to existing methods.

In summary, the following are findings from this study:

- DPI affects the effectiveness of regulator tap operations.
- The magnitude of local renewable/alternative resources affects the DPI that regulators encounter.
- Reverse power flow caused by excessive renewable generation leads to a previously weak source controlling the previously strong source. The downstream toward DER starts controlling the upstream—i.e., the substation side—thus reducing the effectiveness of regulator operations.
- During reverse power flow conditions, the secondary tap-delta reduces, and the primary winding increases in voltage drop (negative tap-delta).

Hypothesis and Future Work

This study focused entirely on developing models for transformers and use cases to aid understanding the impact of DPI on voltage-regulator tap-change effectiveness. The following list mentions a few aspects that we could not complete in this study and that we will focus on in the later part of the ongoing work:

1. The results depict that controlling the low DPI side provides a high tap-delta when compared to controlling the high DPI side; however, the area that needs more work is when both sides of a voltage regulator have similar DPIs. Future work will take a closer look into this.
2. With reference to Figure 9, we expected the primary and secondary tap-delta to be -0.5 and 0.5, respectively, for a DPI ratio of unity; however, the results did not match our expectations, and the primary and secondary tap-delta were -0.5 and 0.5, respectively, for the DPI ratio of 8. We will take a closer look into this in future work.
3. With reference to Figure 9, in an ideal transformer (without losses), the red bar and blue bar are expected to add up to unity; however, the results in Figure 9 do not add up to unity. The missing component is the losses that occur in the transformer windings. These losses are exaggerated by the use of an isolation transformer in the modeling; however, in the field, there are autotransformers, and it is expected that the losses are less. Going forward, if the model requires an isolation transformer, it will be scaled to provide an analogue for the performance of an autotransformer.

Glossary

Driving point impedance	Driving point impedance (DPI) is identical to the positive-sequence impedance for static feeder operation conditions. The DPI is equivalent to the sequence impedance that a voltage regulator encounters in real time. The DPI constantly varies along with the load and PV generation on the feeder. Varying renewable generation and loads affect the DPI that a transformer encounters during daily operation.
Photovoltaic penetration (%)	Photovoltaic (PV) penetration is a relative number with a unit of percentage (%) that represents the aggregate PV generation in a distribution feeder. The PV penetration in this report is a percentage of the peak load on the distribution feeder under analysis
Strong source/weak source	An ideal strong source—i.e., an infinite bus—is a source of invariable frequency and voltage (both in voltage magnitude and angle) with very high fault currents. The opposite of a strong source is a weak source. Weak sources have sensitive voltages and low fault currents. Higher fault currents are caused by strong sources that have low DPI. On the contrary, weak sources have high DPI, leading to low fault currents.
Tap-delta	The tap-delta represents the voltage change per tap. It is typical that the transformer's taps are adjusted in discrete steps, with each step changing the tap ratio by 0.625% (hence a 10% change requires 16 steps). Because of the varying voltage drops caused by changing loads, load tap changers/line regulators are operated in automatic mode The factor tap-delta represents the effectiveness of regulator operation. This term tap-delta has a per unit that ranges from 0–1. A value of 1 represents that a change leads to a 100% (0.625%) expected voltage change, whereas a value of 0.5 represents 50% of expected voltage change. Reduced tap-delta leads to higher tap position, thus leading to higher voltage at the transformer terminal. This can lead to more reactive power flow toward to the load in certain conditions.
Load tap changer	In this report, load tap changers refer to the voltage-regulating controls specific to transformers located at distribution substations.
Line regulator	Line regulators refer to the voltage-regulating controls on transformers with the same voltage class on the primary as well as secondary.

References

1. E.T. Jauch, “Maximizing Automatic Reverse Power Operations with LTC Transformers and Regulators,”" *Power Engineering Society Inaugural Conference and Exposition in Africa* (2005).

2. E.T. Jauch, “How Tapchanger Controls Contribute to Premature Transformer Failures,” *2007 IEEE Power Engineering Society General Meeting Proceedings* (2007): 1–5.

3. E.T. Jauch, “Control Practices Contribute to Premature Transformer Failures,” *IEEE Power Engineering Society Conference and Exposition in Africa—Power Africa Proceedings* (2007): 1–6.

4. G.A. Gilberto and D. Nuñez-P. “Electrical and Magnetic Modeling of a Power Transformer: A Bond Graph Approach,” *World Academy Science Engineering Technology* 6.9 (2012): 591–597.

5. “PLECS: Simulation Software for Power Electronics,” Plexim, http://www.plexim.com.

6. A. Nagarajan, A. Nelson, K. Prabakar, A, Hoke, M. Asano, R. Ueda, and S. Nepal, “Network Reduction Algorithm for Developing Distribution Feeders for Real-Time Simulators,” *IEEE Power and Energy Society General Meeting Proceedings* (2017): 1–5.

Appendix: Modeling SMUD Distribution System

This section describes the process involved in the model conversion from Synergi to OpenDSS. A brief description about the characteristics of the selected feeders is provided prior to details about the model conversion [6].

Synergi-to-OpenDSS Conversion

The Sacramento Municipal Utility District (SMUD), partner utility, identified a distribution feeder for the purpose of studying the impacts of photovoltaic (PV) generation of driving point impedance (DPI) and load tap changer (LTC) operation. The identified feeder is referred to as G011204. The selected feeder has a peak load of 5 MW and 3 MW of PV penetration. The characteristics of the selected feeders are listed in Table A-1. .

Table A-1. Characteristics of Selected Feeder

Components	G011204
Feeder length	11 miles
Peak load	5 MW
Capacitor banks	2
PV generation	3 MW
Node count	4160

Model Conversion

The distribution feeder selected by SMUD, circuit G011024, was converted from Synergi to OpenDSS. The geographical view of the Synergi and OpenDSS models are shown in Figure A-1.

The Synergi-to-OpenDSS conversion uses an automated Python script that takes the network configuration (.xml) and line configuration (.txt) as input. To use the tool, the feeder model provided by SMUD in Microsoft access database format was opened in Synergi and then exported in Extensible Markup Language (XML) format. Additionally, the line impedance information was extracted from Synergi using the Line Construction report and used as an input by the tool. The conversion tool takes the two files described (the feeder in XML format and the line construction report in text format) as inputs and creates a folder with the OpenDSS files. The user can then open the master circuit file and run it in OpenDSS.

The conversion software code is programmed in Python and is structured such that properties for each instance of a Synergi object are collected for all objects in the feeder file in XML format and then operated on via syntax or mathematical conversion to create a corresponding OpenDSS element, associated DSS file, and master circuit file.

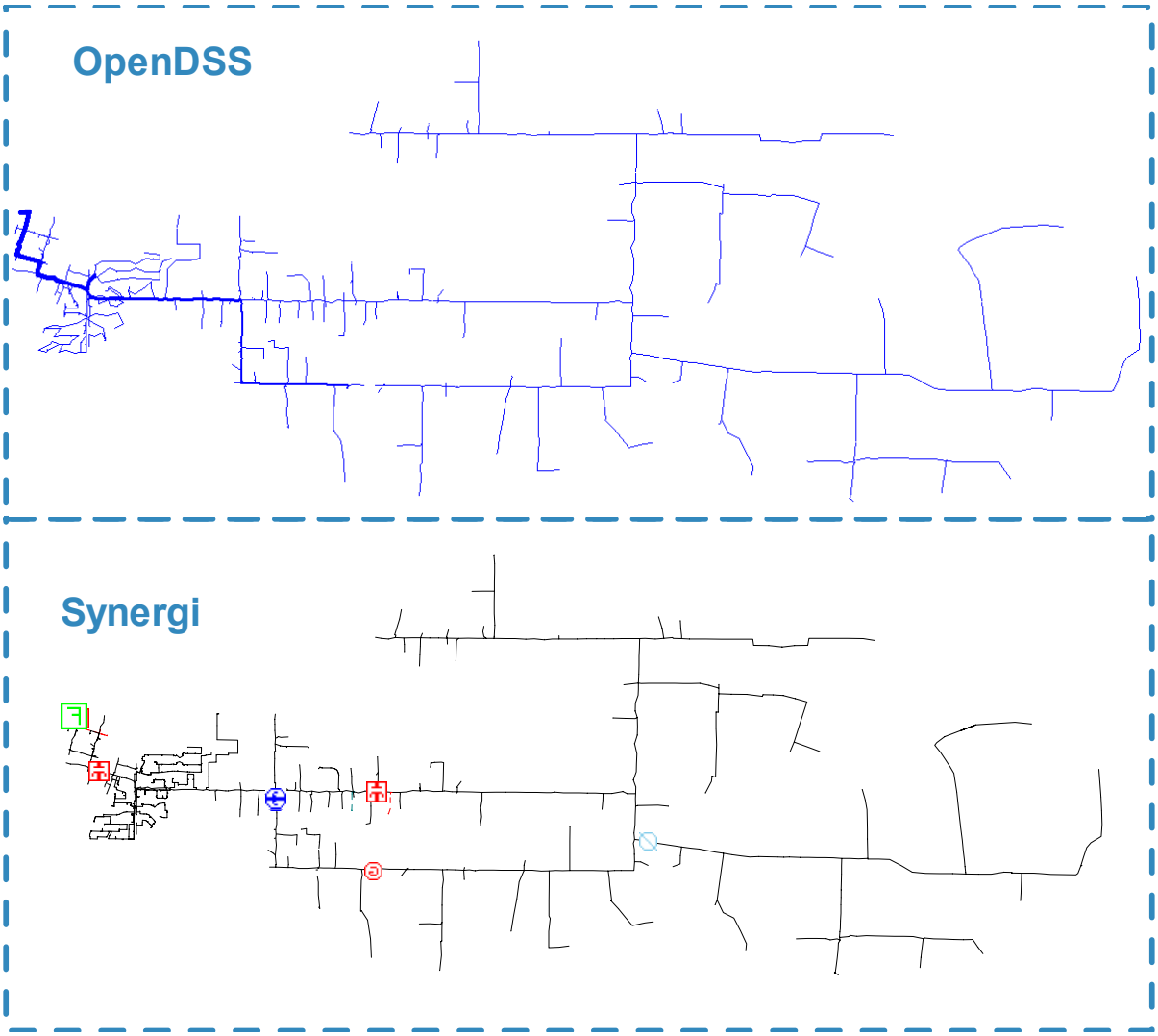

Figure A-1. Geographical view of K3L distribution feeder in Synergi and OpenDSS

Specifically, the conversion process reads the XML file and identifies, collects, and categorizes objects and their parameters for all object blocks within the XML file. As shown in Figure A-2., the object blocks are identified by the symbol "<" with six space characters of indentation from the margin. After the object type is identified, a function defined for that object type is called, and the values for each property are collected. The called function then assigns the collected property values to the container for that object type. In the functions, the values are not altered, and the names of each object are kept the same as those assigned in the Synergi XML file, which assists in the debugging process. The next step in the conversion process is to create objects in the OpenDSS script using the collected Synergi objects and their properties. A view of the syntax identification process is presented in Figure A-2..

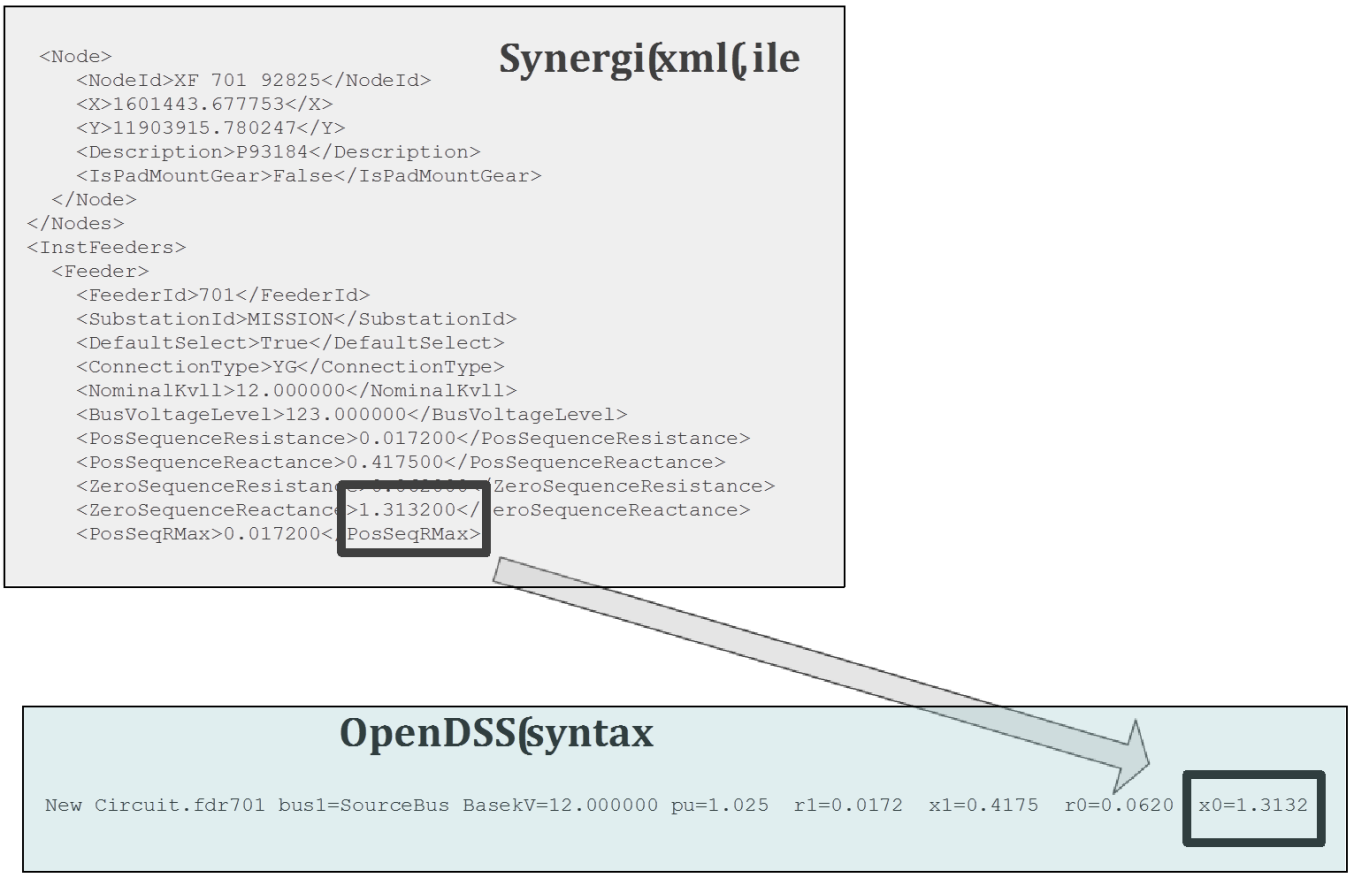

Figure A-2. Diagrammatic view of the Synergi-to-OpenDSS model conversion depicting the syntax identification process

The process of converting objects in Synergi to the equivalent objects in the OpenDSS script is not always a direct one-to-one conversion. Object types that exist in Synergi do not always exist in OpenDSS and vice versa. This is also true for the properties of objects. Switches, reclosers, and fuses are not separate objects in OpenDSS. The conversion tool creates short, low-impedance lines with switching capabilities for these components.

Finally, the converted OpenDSS script is written to a master file, and separate DSS files for each object type are created. The master file initiates a new circuit that creates a voltage source and source bus. The voltage and source impedances are specified based on data from the Synergi model. The master file also redirects to the DSS component files containing scripts for the different object types separated into different categories.

OpenDSS Model Verification

The verification of the OpenDSS model was performed based on the following metrics:

- The feeder topology for the converted model is similar to the original Synergi model based on visual inspection.
- The difference between the node voltages for the converted model and the original Synergi model are less than 1%.

Figure A-1. shows the feeder topology in Synergi and the converted model in OpenDSS. As shown, the line distances and coordinates are appropriately converted. The subsequent step for

verification will compare the voltages obtained from OpenDSS with the Synergi voltages. Figure A-3. and Figure A-4. show the voltage profiles and voltage errors (obtained at full load) as a function of distance and as a histogram.

As shown, the voltage errors are less than 1%; and, as is typical, the voltage errors increase toward the end of the feeder. Although the maximum error is 0.5%, the number of occurrences of errors more than 0.15% is low, as shown in Figure A-3.. Approximately 90% of the node voltage errors are less than 0.15%.

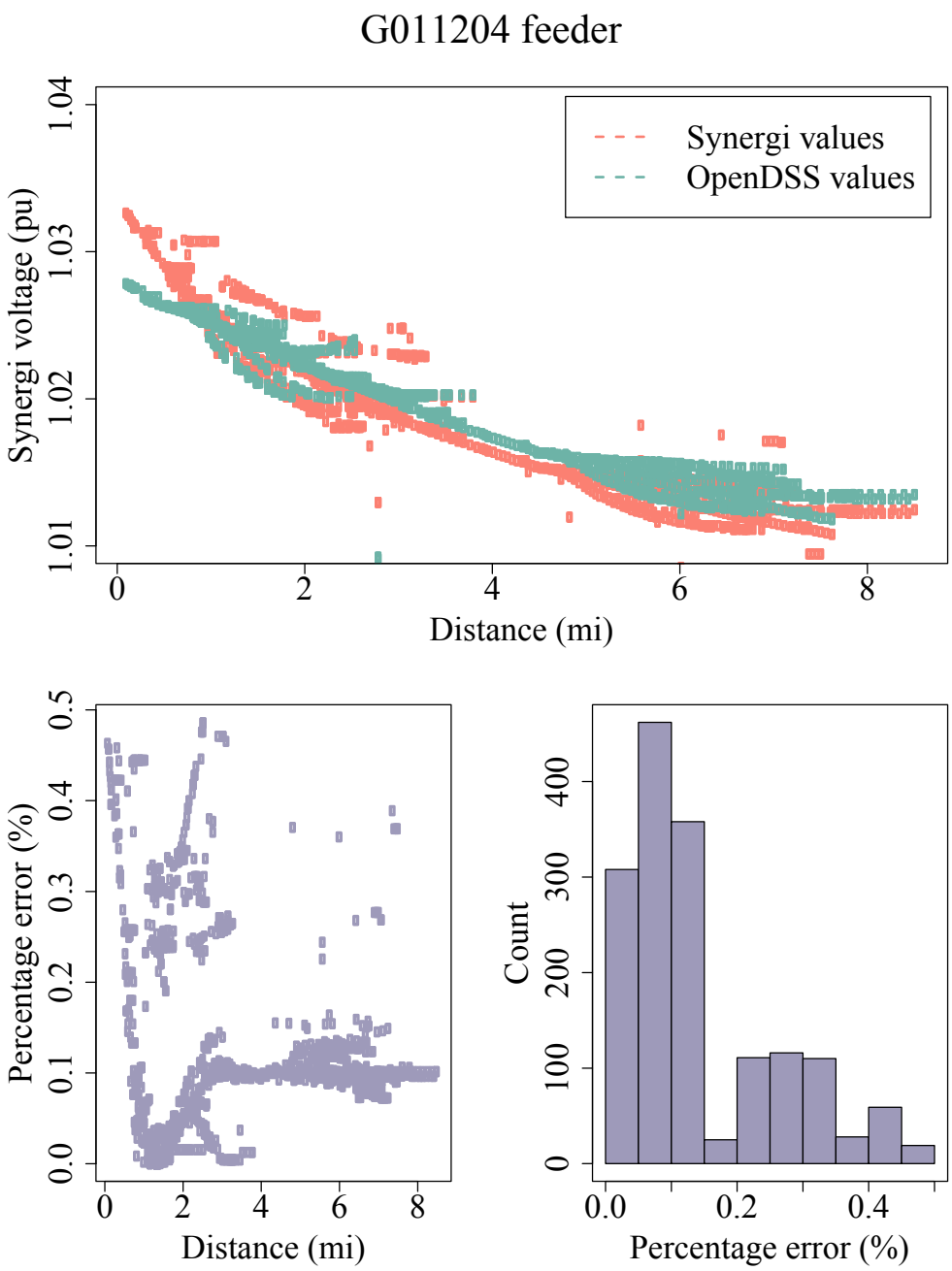

Figure A-3. Percentage error of voltage with respect to distance from the feeder head for the G011204 feeder

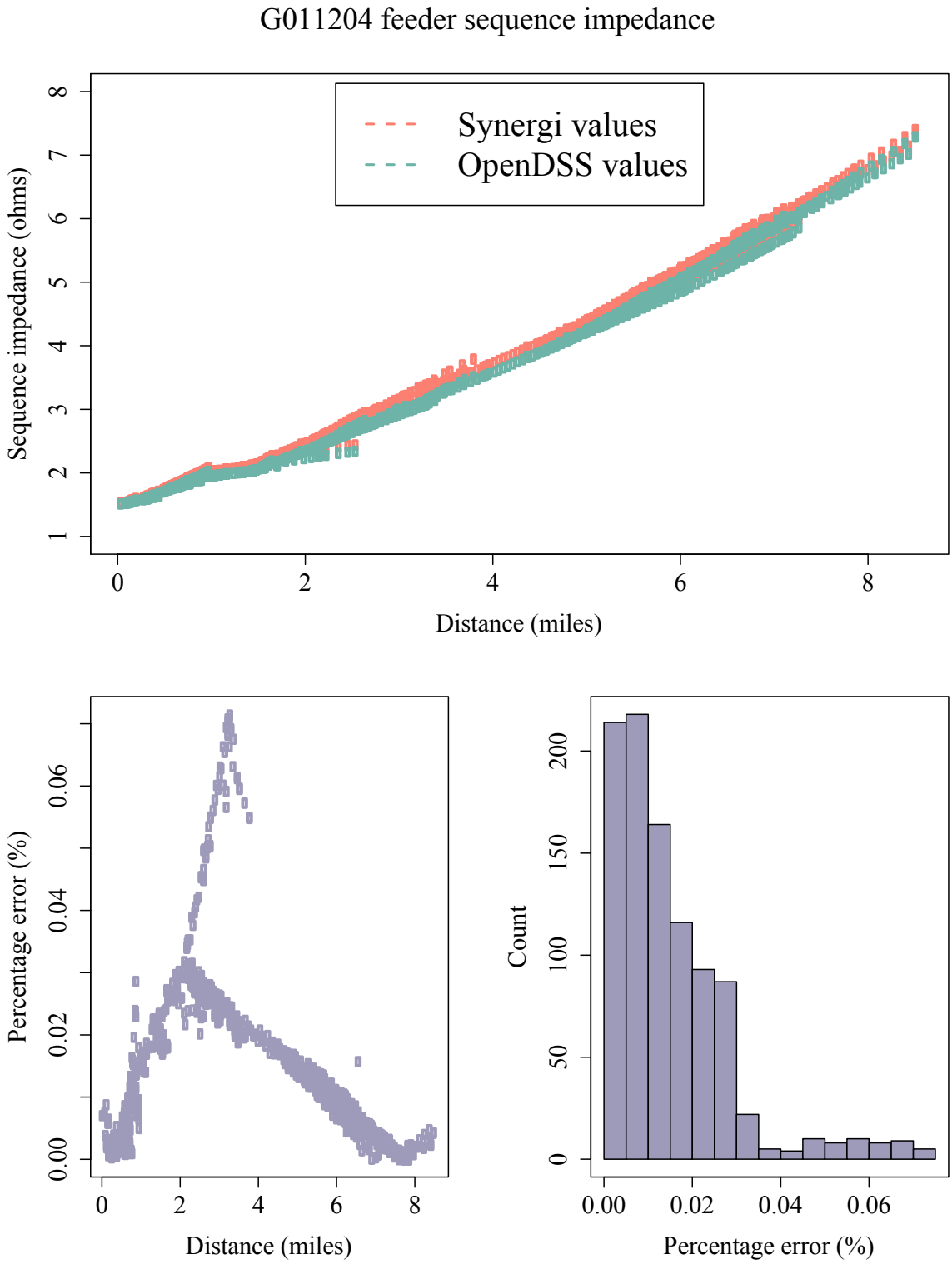

Figure A-4. Percentage error of sequence impedances with respect to distance from the feeder head for the G011204 feeder

Network Reduction

Because the PLECS transient simulation engine, which will be used for the power hardware-in-the-loop experiments, cannot solve the entire network model of a few thousand nodes, a reduced-order model was developed [6].

Model-Reduction Methodology

The original feeder with approximately 4,000 nodes was reduced to 6 nodes using an iterative bottom-up approach in which the user chooses the nodes to be retained. Figure A-5. shows the nodes that were retained.

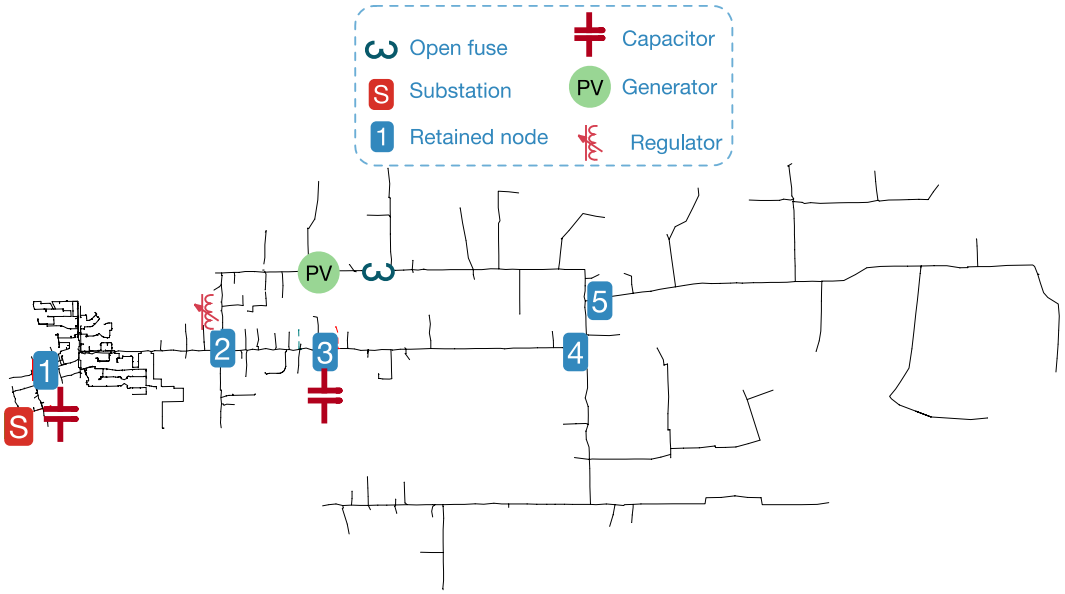

Figure A-5. View of the original feeder with the nodes that were retained

The model-reduction process runs up to 50,000 Monte Carlo simulations, varying line lengths based on a random number generator. The algorithm identifies the combination of line lengths for all lines for which the voltage errors are at a minimum. Figure A-6. diagrammatically outlines the process of network reduction.

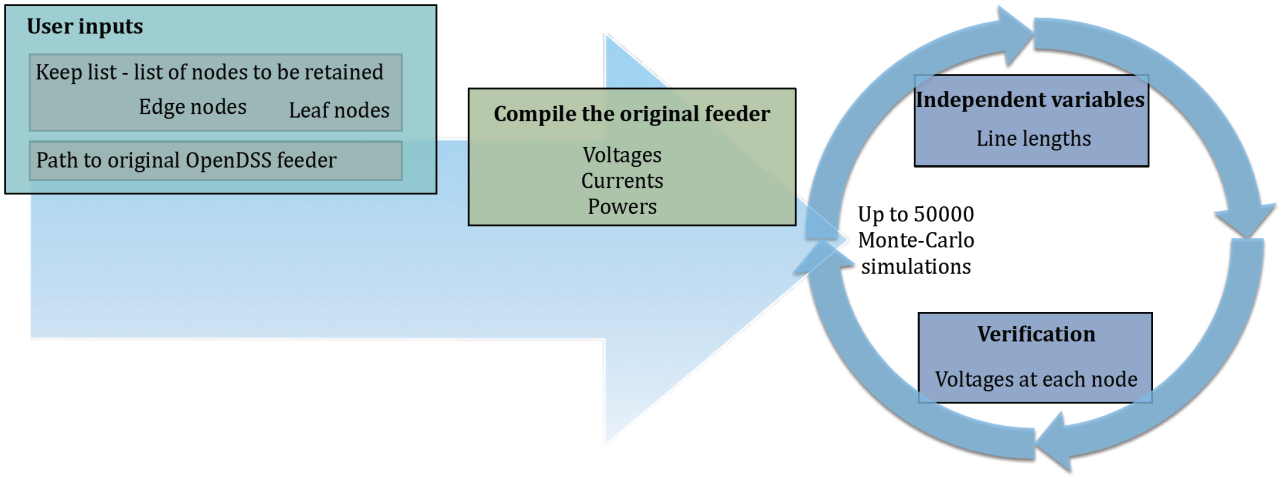

Figure A-6. Outline of network reduction process

Reduced-Order Model Verification

This section verifies the accuracy of the reduced feeder models by comparing the reduced feeder voltages to the original Synergi and OpenDSS models. To ensure that the reduced feeder is good for all load levels, the voltages for 100%, 75%, and 50% loads are compared. The comparison was done with the capacitor banks off and the load set to the peak load, 75% peak load, and 50% peak load. The voltages at the retained nodes for both feeders, along with the error in voltages, are presented in Figure A-7., and results are tabulated in Table A-2.

Table A-2 presents the averaged three-phase voltages at each retained node for the G011204 feeder. Additionally, the retained node voltages are compared to the original OpenDSS model. The percentage errors for each retained node at different loading conditions are presented as well. Table A-2 tabulates the voltages for each phase and each retained node for G011204 feeder. This table compares the voltages of the reduced feeder to the original Synergi model.

The reduced G011204 feeder when compared to the original OpenDSS model (Figure A-7.) had a maximum error of 0.4%. The reduced G011204 feeder when compared to the Synergi model (Table A-2) had a maximum error of 0.7%.

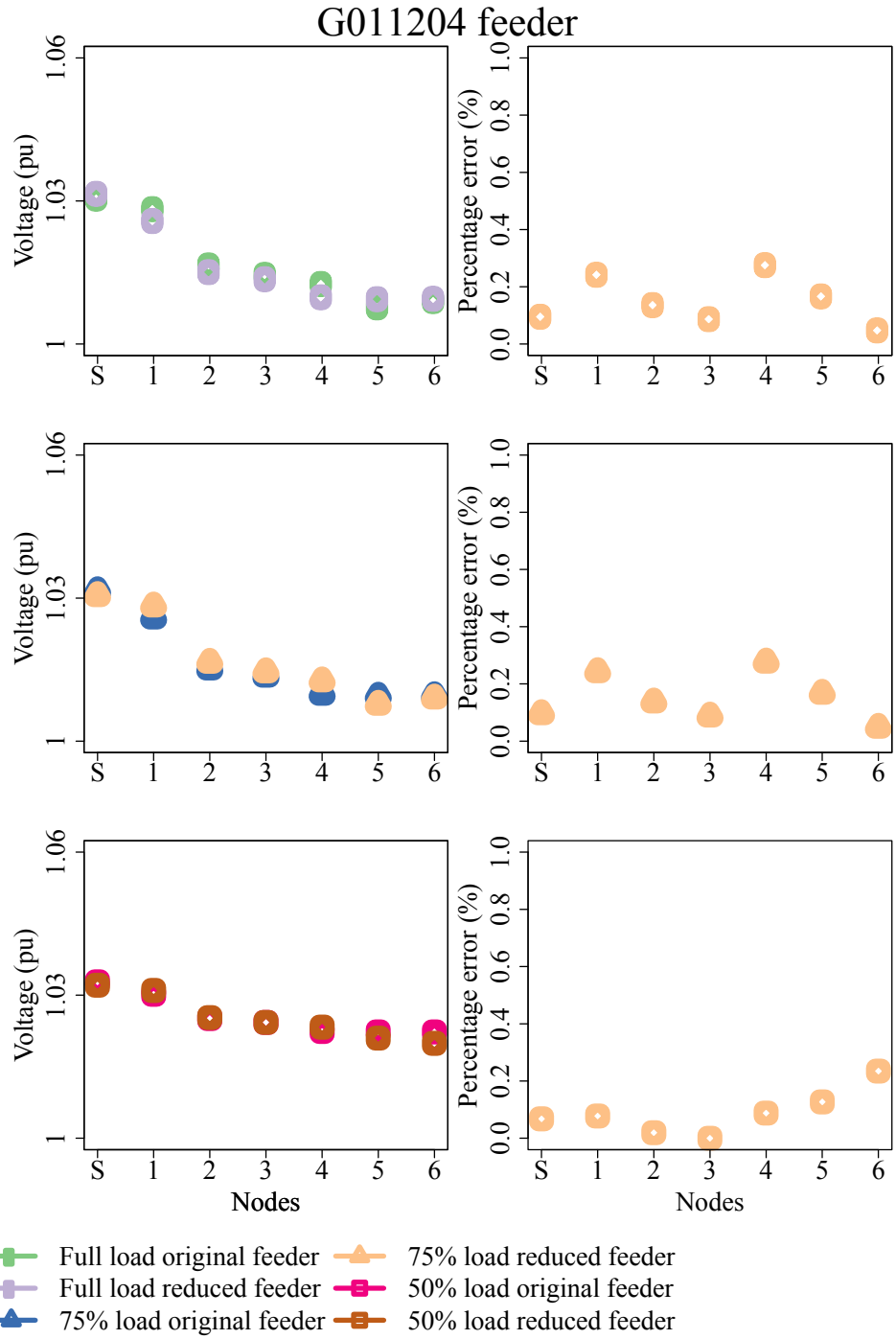

Figure A-7. Voltages at the retained nodes for the reduced-order OpenDSS model and the original OpenDSS model for the G011204 feeder at different loading levels

Table A-2. Voltage Comparison between the Synergi Model and Reduced-Order OpenDSS Model for G011204 Feeder

Nodes	Original Feeder	Reduced Feeder	Error (%)
SOURCEBUS	1.0316	1.0306	0.096936797
	1.0289	1.0282	0.068033823
	1.0258	1.0244	0.136478846
DEV_7642413	1.0259	1.0284	0.243688469
	1.0216	1.0262	0.45027408
	1.0132	1.0112	0.197394394
DEV_7641405	1.0152	1.0166	0.137903861
	1.0084	1.0138	0.535501785
	0.99702	1	0.298890694
NODE_7394816	1.0137	1.0146	0.088783664
	1.0065	1.0118	0.526577248
	0.99449	1.0014	0.694828505
NODE_7372970	1.0099	1.0127	0.277255174
	1.0027	1.0099	**0.718061235**
	0.9901	0.992	0.191899808
NODE_7372964	1.0095	1.0078	0.168400198
	1.0023	1.0053	0.299311583
	0.98972	0.99422	0.454674049
DEV_7575259	1.0096	1.0051	0.445721078
	1.0024	1.0023	0.009976057
	0.98978	0.99127	0.150538504

Modeling the Reduced Feeder in PLECS

The reduced feeder that was developed and validated in the previous sections was modeled in PLECS, a transient analysis tool. For the dynamic DPI analysis, the OpenDSS reduced-order model produced using the procedure in Section 3 was translated into PLECS. Voltage control and PV generator models were added to the reduced feeder model based on data provided by SMUD. This resulted in a complete transient model of the feeder G011204 populated with voltage control devices (voltage regulators and capacitors) and PV inverters. The transient models developed in PLCES were run to perform the suite of experiments discussed in the next section.

Feeder Model Conversion to Real-Time Simulators

The first step in the transient model development was to translate the reduced OpenDSS feeder models into PLECS using the model library. The outputs from the OpenDSS feeder reduction described above include the source impedance parameters, line lengths between nodes, line impedances between nodes, and loads at each node. The feeder-head voltage source was an ideal three-phase voltage source behind a three-phase resistive-inductive source impedance; the voltage source was set for 6.92 kV (line-to-neutral) operating at 60 Hz. The feeder-head voltage was scaled to 103% of nominal for many tests that were required to create overvoltage scenarios. A network of six nodes on the primary was created using resistive-inductive line impedances with the spatial layout following that depicted in Figure A-8. (repeated here as Figure A-7. for convenience). Each node also contained a local, three-phase, unbalanced real and reactive power (PQ) load; each load was based on maximum daily values, so each contained a programmable scaling factor that could be used as an input parameter to adjust load levels for different test cases. When setting up each test, the load scaling factor was adjusted to a value between the feeder's peak load and its gross minimum daytime load. Each load represented an aggregate of the load on each phase in that location in the full feeder model.

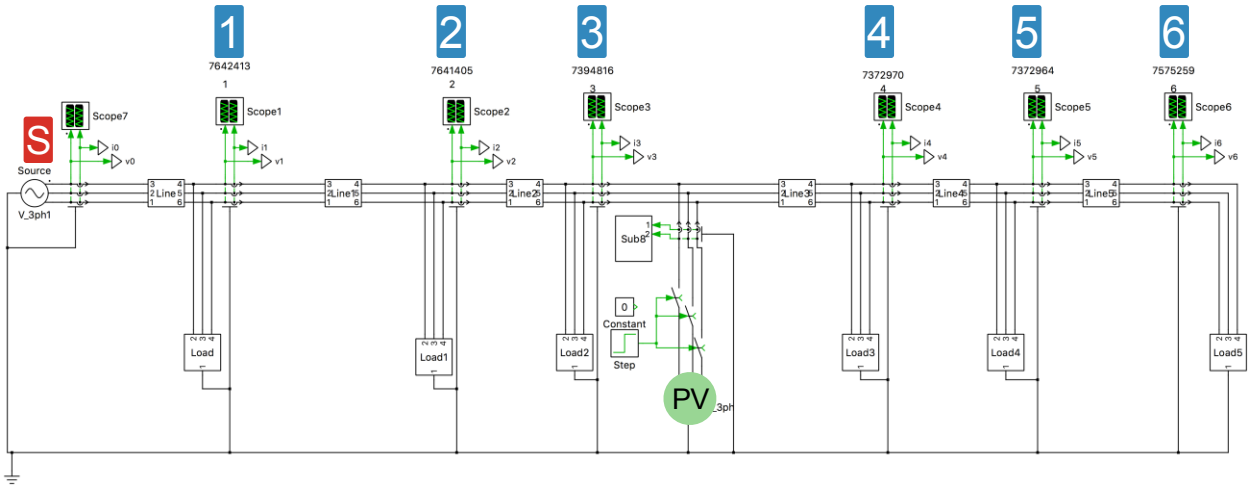

Figure A-8. Model of the reduced feeder schematic as developed in PLECS

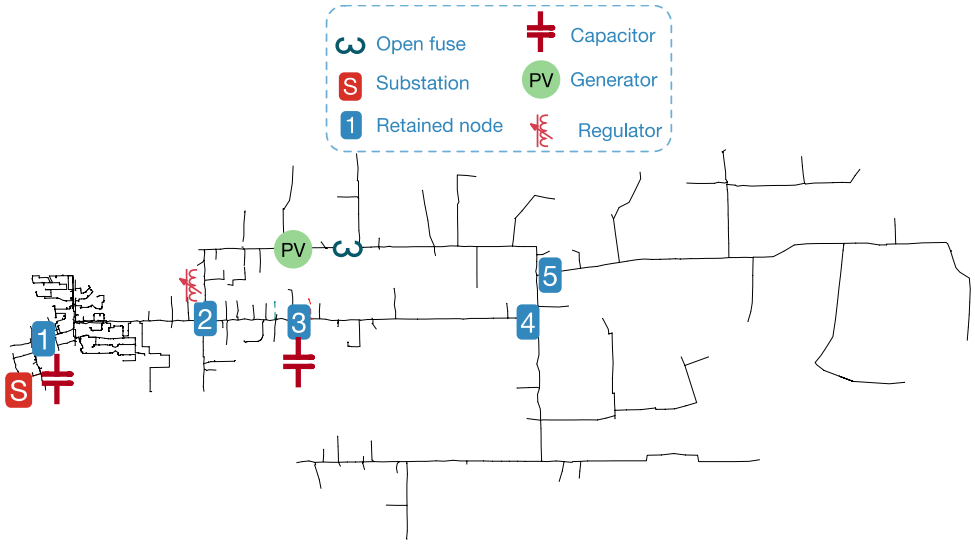

Figure A-9. View of the original feeders with the nodes that were retained

OpenDSS-to-PLECS Model Comparisons

After the reduced-order model parameters were loaded into the PLECS model, all node voltages were manually verified to be the same as the reduced-order OpenDSS model voltages for each phase. For further comparison between the two model types, node voltage comparisons were made between the two models for different PV penetration scenarios. The G011204 feeder model was tested with PV scaled to 100% of fully rated power. The load scale factor was set to 1 (gross daytime minimum load for that feeder), and the source voltage was set to 103% of nominal. Figure A-10. shows the comparison of voltages on each phase at each of the primary nodes under the three test scenarios. As shown, the maximum error for any of these voltages was 0.5%, and the mean error among all voltages was 0.26%.

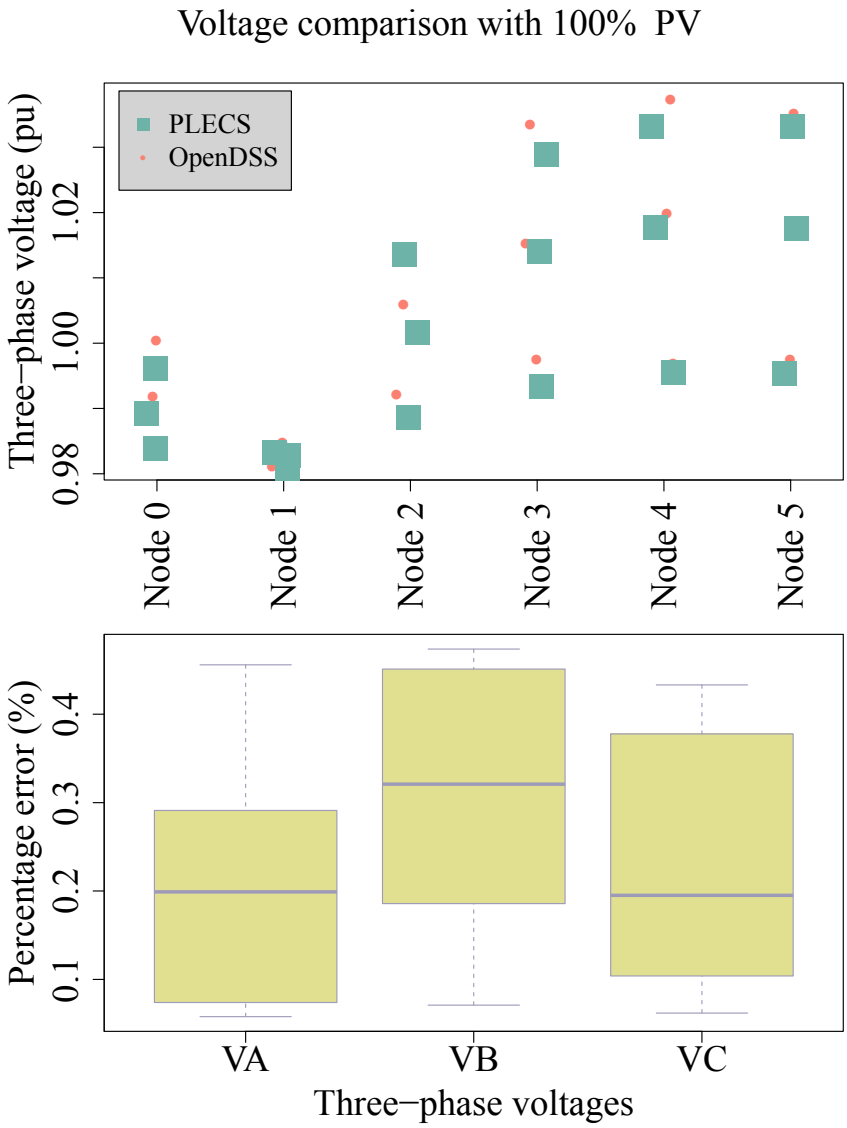

Figure A-10. Comparison of phase voltages between reduced-order OpenDSS model and PLECS model for 100% PV inverter output power on the G011204 model